Article

Antidepressant Effects of (S)-Ketamine through a Reduction of Hyperpolarization-Activated Current I_h

Dorsal CA1 Neuron

Unstress Group

Low I_h Soma

High I_h Dendrite

(S)-ketamine

↓ Dendritic I_h

APs

Saline Pretreatment → ← (S)-ketamine Pretreatment

Chronic Stress

Neuropathological State

↓ Somatic I_h

(S)-ketamine

↓ Dendritic I_h

High I_h

High I_h

Normal-like State

Low I_h

High I_h

Chung Sub Kim,
Daniel Johnston

ckim5@augusta.edu

HIGHLIGHTS

(S)-ketamine reduced the CUS-induced upregulation of somatic I_h

This was independent of NMDAR, Ba^{2+}-sensitive conductances, and cAMP signaling

(S)-ketamine pretreatment before the onset of depression provided resiliency to CUS

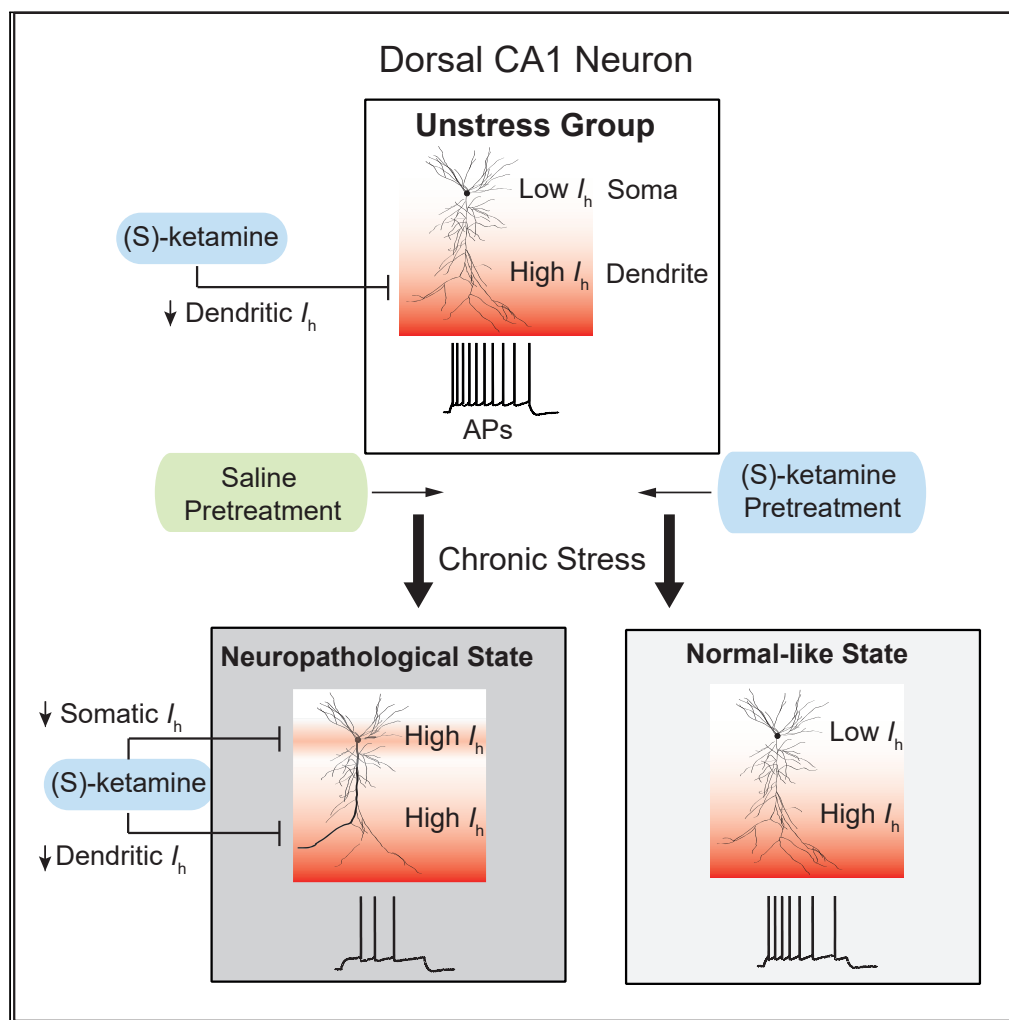*In vivo* thapsigargin-induced changes in behaviors were reversed by (S)-ketamine

Article

Antidepressant Effects of (S)-Ketamine through a Reduction of Hyperpolarization-Activated Current I$_h$

Chung Sub Kim[1,2,*] and Daniel Johnston[1]

SUMMARY

Compelling evidence suggests that a single sub-anesthetic dose of (R,S)-ketamine exerts rapid and robust antidepressant effects. However, the cellular mechanisms underlying the antidepressant effects of (R,S)-ketamine remain unclear. Here, we show that (S)-ketamine reduced dendritic but not somatic hyperpolarization-activated current I$_h$ of dorsal CA1 neurons in unstressed rats, whereas (S)-ketamine decreased both somatic and dendritic I$_h$ in chronic unpredictable stress (CUS) rats. The reduction of I$_h$ by (S)-ketamine was independent of NMDA receptors, barium-sensitive conductances, and cAMP-dependent signaling pathways in both unstressed and CUS groups. (S)-ketamine pretreatment before the onset of depression prevented CUS-induced behavioral phenotypes and neuropathological changes of dorsal CA1 neurons. Finally, *in vivo* infusion of thapsigargin-induced anxiogenic- and anhedonic-like behaviors and upregulation of functional I$_h$, but these were reversed by (S)-ketamine. Our results suggest that (S)-ketamine reduces or prevents I$_h$ from being increased following CUS, which contributes to the rapid antidepressant effects and resiliency to CUS.

INTRODUCTION

Depression is a life-threatening mental illness with a prevalence rate of about 4.7% worldwide (Ferrari et al., 2013; Bostwick and Pankratz, 2000). Current monoaminergic antidepressants show limited effects such as delayed onset and partial efficacy, leading to an increase in risk of suicidal behavior. Unlike monoaminergic antidepressants, a single sub-anesthetic dose of (R,S)-ketamine, an NMDA receptor antagonist, has been shown to have rapid and sustained antidepressant effects in treatment-resistant depression (TRD) (Berman et al., 2000; Zarate et al., 2006a). However, the mechanism underlying the antidepressant effect of (R,S)-ketamine remains unclear. Although there has been controversy over (R,S)-ketamine's NMDA receptor-dependent or NMDA receptor-independent antidepressant effect (Preskorn et al., 2008; Lodge and Mercier, 2015; Zarate et al., 2006b; Zanos et al., 2016; Suzuki et al., 2017), the antidepressant effect is, in general, associated with (1) increases in brain-derived neurotrophic factor (BDNF)-mammalian target of rapamycin (mTOR) signaling pathway, (2) a decrease in eukaryotic elongation factor 2 (eEF2) kinase, and (3) increases in synaptogenesis, spine density, and α-amino-3-hydroxy-5-methyl-4-isoxazole-propionic acid (AMPA) receptor expression (Li et al., 2010; Autry et al., 2011; Maeng et al., 2008).

Hyperpolarization-activated cyclic nucleotide-gated nonselective cation (HCN) channels are highly expressed in the hippocampus, cortex, and cerebellum (Monteggia et al., 2000). HCN1 is the main isoform of HCN channels (HCN1–HCN4) and is highly expressed in the hippocampal CA1 region with a gradient of increasing channel expression along the somatodendritic axis (Lorincz et al., 2002; Magee, 1998). HCN channels are active at the resting membrane potential, which contributes to the intrinsic membrane properties of neurons (e.g., resting membrane potential, input resistance [R$_{in}$], resonance frequency [f$_R$], neuronal excitability, and synaptic integration; Narayanan and Johnston, 2007; Kim et al., 2012; Magee, 1999). We previously showed that knockdown of the HCN1 subunit in the dorsal CA1 region of the hippocampus, which corresponds to the posterior hippocampus in humans, produces anxiolytic- and antidepressant-like behaviors in unstressed rats (Kim et al., 2012). These changes in behaviors are associated with an increase in neuronal excitability, an enhancement of BDNF-mTOR signaling, an increase in synaptic excitation, and an increase in dorsal hippocampal activity (Kim et al., 2012). We also recently reported that

[1]Center for Learning and Memory and Department of Neuroscience, University of Texas at Austin, 1 University Station Stop, C7000, Austin, TX 78712, USA

[2]Lead Contact

*Correspondence: ckim5@augusta.edu

https://doi.org/10.1016/j.isci.2020.101239

HCN1 protein expression and I_h are increased in the perisomatic region of dorsal hippocampal CA1 following chronic, but not acute stress (Kim et al., 2018). A reduction of HCN1 protein expression in the dorsal CA1 region before the onset of CUS produces resiliency to CUS (Kim et al., 2018). Furthermore, *in vivo* block of the sarcoplasmic/endoplasmic reticulum Ca^{2+}-ATPase (SERCA) pumps in dorsal CA1 region produces anxiogenic-like behaviors in the open field test and upregulation of functional I_h, similar to that observed in rats following CUS (Kim et al., 2018).

It has been reported that (S)-ketamine, the S enantiomer of (R,S)-ketamine, inhibits HCN1-mediated I_h via a hyperpolarization shift in voltage dependence of activation and a reduction of total I_h conductance in layer 5 cortical pyramidal neurons in unstressed conditions (Chen et al., 2009). Moreover, the US Food and Drug Administration (FDA)-approved intranasal (S)-ketamine shows a rapid antidepressant effect among patients with TRD and decreases suicide ideation in major depression (Canuso et al., 2018). Given that knockdown of HCN1 and treatment with (R,S)-ketamine activate similar downstream signaling pathways (e.g., increased BDNF-mTOR signaling) and produce similar behavioral outcomes (e.g., anxiolytic- and antidepressant-like behaviors) (Kim et al., 2012; Autry et al., 2011; Li et al., 2010), we sought to investigate whether (1) (S)-ketamine changes I_h in the dorsal CA1 neurons and (2) (S)-ketamine pretreatment before the onset of depression exerts resiliency to CUS.

In this study, we found that S-ketamine reduced dendritic but not somatic I_h in normal or unstressed conditions. Using the CUS model of depression, however, we found that (S)-ketamine reduced not only dendritic but also the CUS-induced upregulation of somatic I_h (Kim et al., 2018). The (S)-ketamine-induced reduction in I_h was due to a decrease in maximal h current and a hyperpolarizing shift to the h channel activation curve. The observed (S)-ketamine-induced reduction in I_h-sensitive electrophysiological measurements (i.e., higher input resistance, R_{in}, and lower resonance frequency, f_R, see Methods) was independent of NMDA receptors, barium-sensitive conductances (e.g., inwardly rectifying K^+ channels), and cAMP-dependent signaling pathways in both unstressed and CUS groups. We show that (S)-ketamine pretreatment before the onset of CUS prevented the CUS-induced abnormal behaviors (i.e., anxiogenic- and depressive-like behaviors) and neuropathological changes (i.e., upregulation of somatic I_h and a decrease in neuronal excitability). Finally, *in vivo* infusion of thapsigargin (TG) followed by infusion of (S)-ketamine showed that TG-induced changes in behaviors (e.g., anxiogenic- and anhedonic-like behaviors) and upregulation of functional I_h (e.g., decreased R_{in} and increased f_R) were reversed by (S)-ketamine.

RESULTS

Changes in Dendritic but Not Somatic I_h following (S)-Ketamine Application in Unstressed Conditions

A single sub-anesthetic dose of (R,S)-ketamine (0.5 mg/kg intravenous [i.v.] infusion for 40 min) exerts rapid and sustained antidepressant effects in major depressive disorder (Berman et al., 2000). Given the similar downstream signaling pathways (e.g., increased BDNF-mTOR signaling) and behavioral outputs (e.g., anxiolytic- and antidepressant-like behaviors) between a reduction of HCN1 protein expression (Kim et al., 2012) and (R,S)-ketamine treatment (Autry et al., 2011; Li et al., 2010), our goal was to investigate whether (S)-ketamine had effects on I_h in dorsal CA1 neurons. We focused on dorsal neurons because (1) knockdown of HCN1 in the ventral CA1 region has no anxiolytic- or antidepressant-like effects and (2) there are no changes in I_h-sensitive electrophysiological measurements (e.g., R_{in} and f_R) of ventral CA1 neurons following CUS (Kim et al., 2018). It is known that (S)-ketamine inhibits HCN1 channels, resulting in a hyperpolarization shift in voltage dependence of activation and a reduction of total I_h conductance in layer 5 cortical pyramidal neurons in unstressed conditions and human embryonic kidney (HEK) 293 cells expressing homomeric mouse HCN1 channels (Chen et al., 2009). A key feature of HCN1 channels is a distance-dependent increase in protein expression (Lorincz et al., 2002) (Figure S1A) and I_h-sensitive measurements (i.e., lower R_{in} and higher f_R, Figure S1B) along the somatodendritic axis of CA1 pyramidal neurons. ZD7288, an HCN channel blocker, reduced I_h-sensitive measurements (i.e., it increased R_{in} and removed f_R, Figure S1C). We performed whole-cell current-clamp recordings at the soma (Figures 1A–1E) and dendrite (Figures 1F–1J), where HCN channels are heavily expressed, and all experiments were done in the presence of glutamatergic synaptic blockers (D-AP5 and DNQX). Somatic R_{in} (Figures 1B–1D) and f_R (Figures 1B, 1C, and 1E) were not significantly altered following bath application of (S)-ketamine (Figure S2). On the other hand, (S)-ketamine significantly increased dendritic R_{in} and decreased dendritic f_R consistent with a reduction of I_h (Figures 1G–1J). In keeping with the known somatodendritic gradient of I_h (Magee, 1998), there was also a correlation between a change (%) in I_h-sensitive measurements (i.e., R_{in} and f_R) and the distance
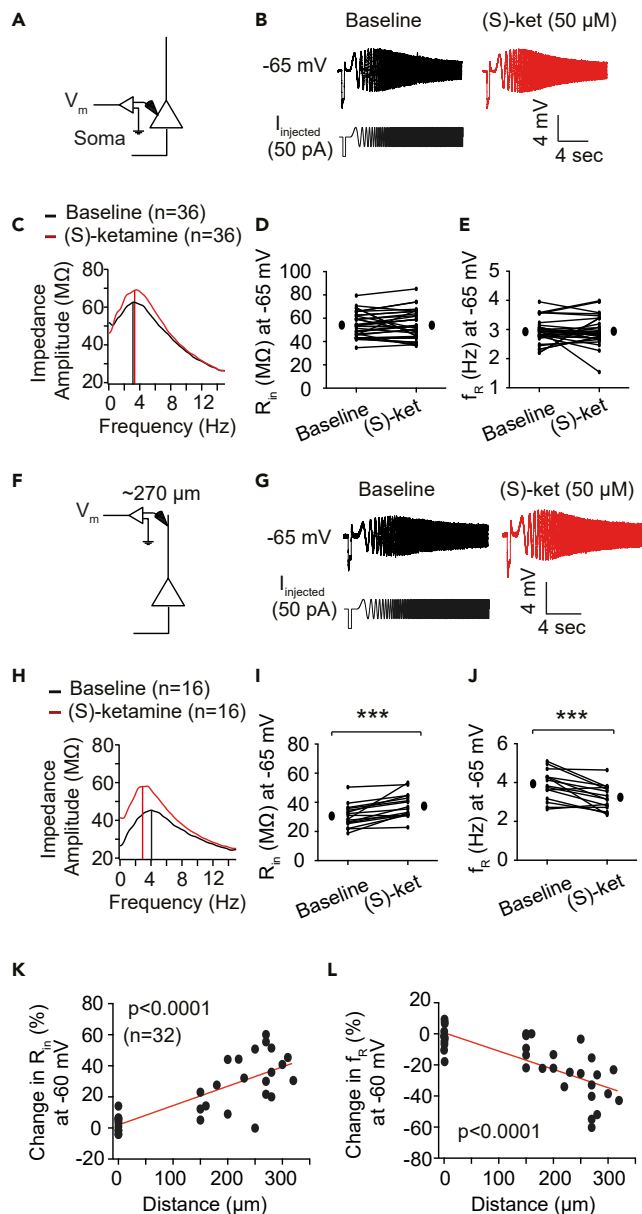
Figure 1. Changes in Dendritic but Not Somatic I_h-Sensitive Electrophysiological Measurements within 10–20 Min Following (S)-Ketamine Application

(A and F) Schematic of the somato-apical trunk depicting the somatic (A) and the dendritic (F) recordings.

(B and G) Representative voltage traces from -65 mV in response to a sinusoidal current injection of constant amplitude and linearly spanning 0-15 Hz in 15 sec.

(C and H) The profile of impedance amplitude for voltage traces in (B and G). Vertical lines indicate the resonance frequencies. Somatic f_R was not significanlty altered following (S)-ketamine application (C), whereas (S)-ketamine significantly reduced dendritic f_R (H).

(D and E) Somatic (D) R_{in} and (E) f_R at −65 mV were not altered following (S)-ketamine application.

(I and J) Dendritic (I) R_{in} and (J) f_R at −65 mV were significantly changed following (S)-ketamine application. ***$p < 0.001$ by Wilcoxon matched-pairs signed rank test.

(K and L) Changes in (K) R_{in} (%) and (L) f_R (%) at −60 mV were distance dependent along the somatodendritic axis of dorsal CA1 neurons following (S)-ketamine application. $p < 0.0001$ by linear regression analysis. Data are expressed as mean ± SEM.
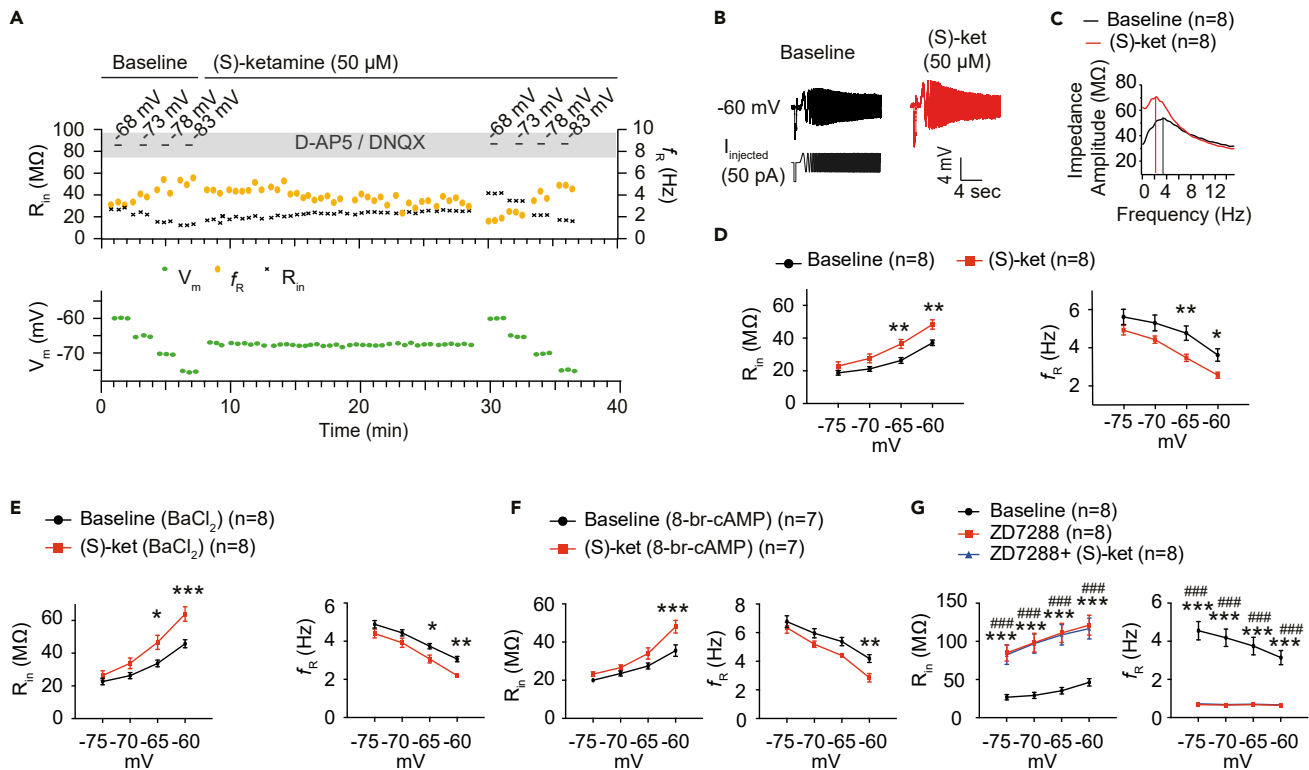
Figure 2. Changes in Dendritic I_h-Sensitive Measures by (S)-Ketamine Were Independent of a Barium-Sensitive Conductance and cAMP-Dependent Signaling

(A) Time courses of changes in V_m, R_{in}, and f_R during (S)-ketamine wash-in experiment in the dorsal CA1 neurons (green: V_m, orange: f_R, and black: R_{in}).

(B) Representative voltage traces and current injections at different membrane potentials (ranging from −60 mV to −75 mV; −5 mV interval).

(C) The profile of impedance amplitude for voltage traces in (B).

(D) Dendritic R_{in} and f_R were significantly changed at depolarized membrane potentials following (S)-ketamine application. *$p < 0.05$, **$p < 0.01$ by two-way ANOVA with Sidark's multiple comparisons test.

(E) Dendritic R_{in} and f_R were significantly changed at depolarized membrane potentials in the presence of barium chloride (25 μM) following (S)-ketamine application. *$p < 0.05$, **$p < 0.01$, ***$p < 0.001$ by two-way ANOVA with Sidark's multiple comparisons test.

(F) Bath application of (S)-ketamine increased dendritic R_{in} and decreased dendritic f_R at depolarized membrane potentials in the presence of 8-bromo-cAMP (100 μM). **$p < 0.01$, ***$p < 0.001$ by two-way ANOVA with Sidark's multiple comparisons test.

(G) The effects of (S)-ketamine were occluded by ZD7288 (10 μM) in the dorsal CA1 neurons. Subsequent bath application of (S)-ketamine (50 μM) had no further effects on dendritic R_{in} and f_R. ***$p < 0.001$ (baseline versus ZD7288) and ###$p < 0.001$ (baseline versus ZD7288+(S)-ket) by two-way ANOVA with Sidark's multiple comparisons test. Data are expressed as mean ± SEM.

from the soma to dendrite (Figures 1K and 1L). We also examined whether the effects of (S)-ketamine on dendritic I_h-sensitive measurements were dose dependent in dorsal CA1 neurons. We used four different concentrations of (S)-ketamine (1, 10, 50, and 100 μM) and measured changes in dendritic R_{in} and f_R at −60 mV. Changes in I_h-sensitive measurements at −60 mV were significantly affected by bath application of either 50 or 100 μM of (S)-ketamine compared with baseline (Figure S3). There was no significant difference between 50 and 100 μM (S)-ketamine (Figure S3). We, therefore, used 50 μM for all our experiments.

The (S)-Ketamine Effect on Dendritic I_h Was Independent of Barium-Sensitive Conductances and cAMP-Dependent Signaling

Given the voltage dependence of HCN channels, we measured dendritic R_{in} and f_R at different membrane potentials (ranging from −60 mV to −75 mV, −5 mV interval) before and after bath application of (S)-ketamine. V_m, R_{in}, and f_R were monitored during (S)-ketamine wash-in in dorsal CA1 neurons (Figure 2A). We consistently observed reduced dendritic I_h-sensitive measurements (i.e., increased R_{in} and decreased f_R) within 10–20 min (Figure 2A). Dorsal CA1 neurons showed increased dendritic R_{in} and decreased dendritic f_R at depolarized membrane potentials (Figures 2B–2D) following bath application of (S)-ketamine. We have previously found that a G protein-coupled inwardly rectifying potassium (GIRK) conductance,

in part, contributes to intrinsic membrane properties (e.g., R_{in} and resting membrane potential) of dorsal CA1 neurons (Kim and Johnston, 2015). We, therefore, examined whether the increased R_{in} following (S)-ketamine application was due to a change in GIRK conductance. Low concentrations of Ba^{2+} (25–50 μM) block inwardly rectifying K^+ channels such as GIRK and IRK (Kim and Johnston, 2015; Malik and Johnston, 2017). Dendritic I_h-sensitive measurements were significantly reduced (i.e., increased R_{in} and decreased f_R) at depolarized membrane potentials in the presence of Ba^{2+} (25 μM) following bath application of (S)-ketamine (Figure 2E), suggesting that its effects were independent of a barium-sensitive conductance (e.g., IRK and GIRK conductances). It has been reported that acute (R,S)-ketamine treatment (10 μM for 15 min) on C6 glioma cells or primary astrocytes increased translocation of $G_{αs}$ from lipid rafts to nonrafts after 24 h, suggesting cAMP-dependent antidepressant action of (R,S)-ketamine (Wray et al., 2018). Because HCN channels have a cyclic nucleotide-binding domain (Wang et al., 2001), we further explored whether the (S)-ketamine-induced reduction of dendritic I_h-sensitive measurements was dependent on cAMP-dependent signaling. 8-bromo-cyclic AMP (cAMP) is a membrane-permeable activator of cAMP-dependent protein kinase. Because we did not observe any changes in intrinsic membrane properties (e.g., V_m, R_{in}, and f_R) of dorsal CA1 neurons following bath application of 8-bromo-cAMP (100 μM) (Figure S4), as a control for 8-bromo-cAMP, we examined whether the applied 8-bromo-cAMP was having the known physiological effects on active properties of dorsal CA1 neurons. It has been reported that back-propagating action potential (bAP) amplitude, which decreases with distance from the soma due to an increased density of A-type K^+ channels, is increased by protein kinase A activation (Hoffman and Johnston, 1998). We, therefore, measured bAPs elicited by antidromic extracellular stimulation in the stratum oriens at the soma, proximal dendrites (∼220 μm from the soma), and distal dendrites (∼320 μm from the soma) (Figures S5A and S5B). Consistent with the report by Hoffman and Johnston (1998) we observed increased bAP amplitude at −65 mV in the distal dendrites of dorsal CA1 neurons following 8-bromo-cAMP, indicating 8-bromo-cAMP-induced physiological effects on dorsal CA1 neurons (Figures S5A and S5B). Bath application of (S)-ketamine led to increased dendritic R_{in} and decreased dendritic f_R at depolarized membrane potentials in the presence of 8-bromo-cAMP (Figures 2F, S5C, and S5D), suggesting that the (S)-ketamine-induced decrease in I_h-sensitive measurements was independent of the cAMP-dependent signaling. Last, we asked whether block of I_h occluded the (S)-ketamine-dependent reduction of dendritic I_h-sensitive measurements in the dorsal CA1 neurons. We performed successive ZD7288 and (S)-ketamine wash-in experiments and measured dendritic R_{in} and f_R at resting membrane potential (RMP) and at different membrane potentials. V_m, R_{in}, and f_R at RMP were monitored during bath application of ZD7288 (10 μM, 4–5 min) and (S)-ketamine (50 μM) (Figure S6A). Bath application of ZD7288 significantly increased R_{in} and abolished f_R at RMP (Figures S6B, S6C, S6E, and S6F) and at different membrane potentials (Figure 2G). Subsequent addition of (S)-ketamine had no further effect on V_m, R_{in}, and f_R at RMP (Figures S6B–S6F) and at different membrane potentials (Figure 2G) in the dorsal CA1 neurons, suggesting that ZD7288 occluded the effect of (S)-ketamine. These results suggested that (S)-ketamine reduced dendritic but not somatic I_h-sensitive measurements independent of NMDA receptors, barium-sensitive conductances, and cAMP-dependent signaling.

The Effect of (S)-Ketamine on Voltage-Dependent Gating of *h* Channel and the Amplitude of *h* Current

We have thus far demonstrated that (S)-ketamine decreased dendritic but not somatic I_h-sensitive electrophysiological measurements at depolarized membrane potentials (Figure 2). To measure directly the effect of (S)-ketamine on I_h, we performed cell-attached patch-clamp recordings from the soma and dendrites of dorsal CA1 neurons in the presence of D-AP5 and DNQX with or without the prior treatment for 30 min of (S)-ketamine (50 μM). We determined voltage-dependent gating of *h* channel and the amplitude of *h* current with 500-ms hyperpolarizing voltage steps ranging from −40 to −170 mV in −10 mV increments from a holding potential of −30 mV (Figures 3A and 3H). Given that somatic I_h was too small to determine the conductance-voltage (G-V) relationship from the peak of the tail current, we constructed a steady-state G-V relationship from the steady-state *h* current in response to each voltage step (Figure 3B). With the solutions used (see Methods) the reversal potential of I_h was experimentally determined from dendritic recordings ($E_h = -10$ mV; data not shown). At the soma, we found that the $V_{1/2}$ of the *h* channel activation curve (Figures 3B and 3C), the slope factor (Figures 3B and 3D), and the maximal I_h at −170 mV (Figures 3E and 3F) were not significantly different between artificial cerebrospinal fluid (ACSF)-treated and (S)-ketamine-treated groups. Steady-state I_h amplitude at different membrane potentials (i.e., I-V curve) was also not different between ACSF-treated and (S)-ketamine-treated groups (Figure 3G), consistent with no measurable effects of (S)-ketamine on current-clamp somatic I_h-sensitive measurements (Figure 1). Dendrites had much larger I_h currents, allowing us to determine the voltage dependence of activation from
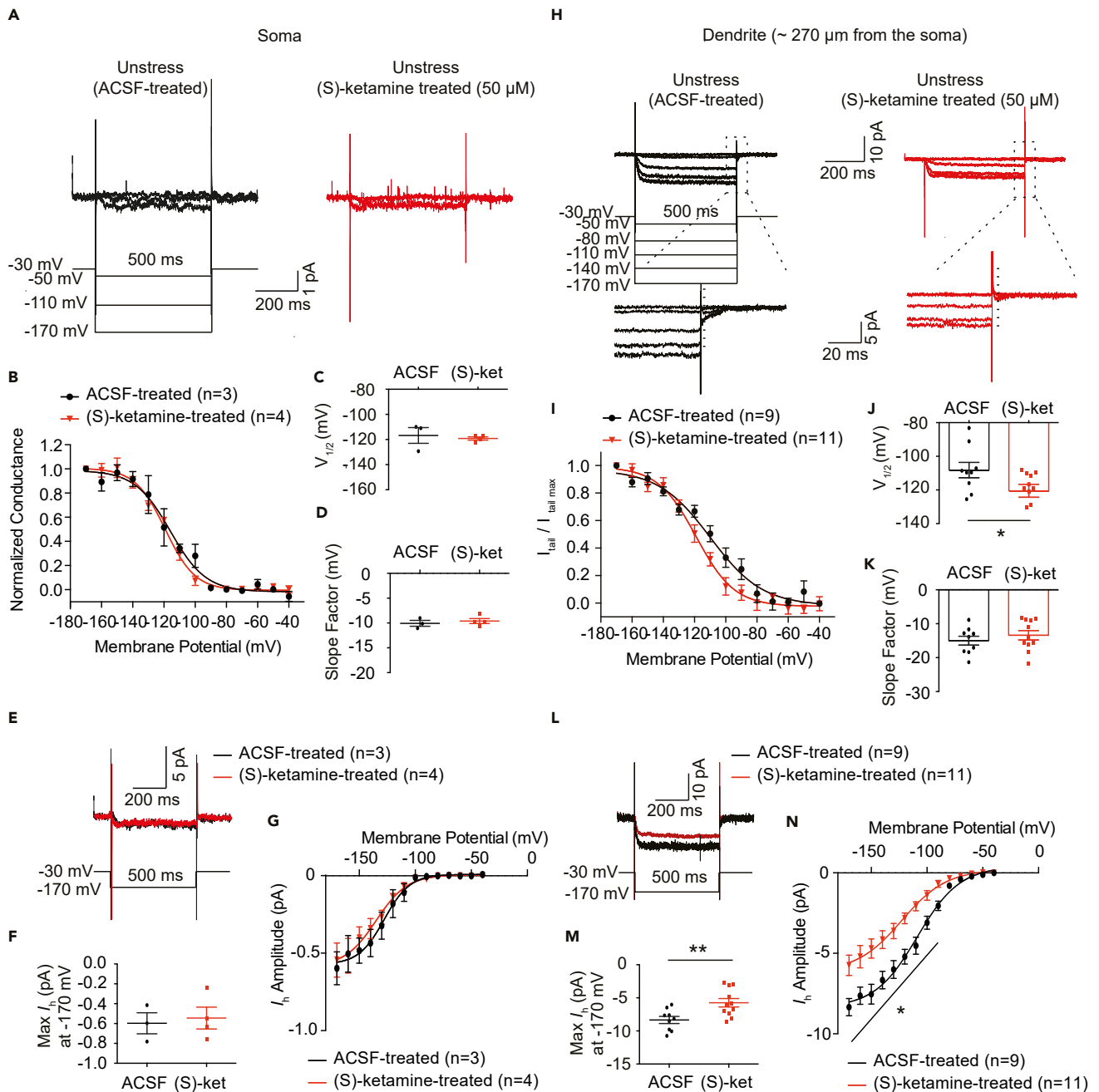
Figure 3. (S)-Ketamine Changed Voltage-Dependent Gating of *h* Channel and the Amplitude of *h* Current in the Dendrites of Dorsal CA1 Neurons

(A and H) Somatic (A) or dendritic (H; ~270 μm from the soma) *h* current was measured using cell-attached patches from dorsal CA1 neurons after ACSF-treated or (S)-ketamine-treated (50 μM, 30 min) slices with 500-ms hyperpolarizing voltage steps ranging from −40 mV to −170 mV in −10 mV increments from a holding potential of −30 mV. Insets in (H): tail currents are enlarged from the dashed box. Vertical dashed lines indicate the location for determining the peak tail current.

(B) The voltage dependence of activation for *h* channel was determined from the somatic steady-state G-V relationship. The activation curve was fitted a Boltzmann function with the following values: ACSF treatment $V_{1/2}$ = −116.8 mV, k = −10.07 mV; (S)-ketamine treatment $V_{1/2}$ = −119.2 mV, k = −9.6 mV.

(C and D) The half-activation voltage ($V_{1/2}$; C) and slope factor (D) were not significantly different between ACSF-treated and (S)-ketamine-treated groups.

(E) Representative maximal *h* current traces in response to a 500-ms hyperpolarizing voltage step (−170 mV).

(F) Maximal somatic *h* current at −170 mV was not different between ACSF-treated and (S)-ketamine-treated groups.

(G) There was no difference in the I-V curve between ACSF-treated and (S)-ketamine-treated groups.

(I) The voltage dependence of activation for *h* channel was determined from tail currents. The activation curve was fitted with a Boltzmann function with the following values: ACSF treatment $V_{1/2}$ = −108.2 mV, k = −15 mV; (S)-ketamine pretreatment $V_{1/2}$ = −120.5 mV, k = −13.4 mV.

Figure 3. *Continued*

(J and K) (J) The half-activation voltage of h channel ($V_{1/2}$) with (S)-ketamine treatment was significantly shifted to the left by around -12 mV, whereas the slope factor (K) was not different compared with those from ACSF-treated group. *p < 0.05 by Mann-Whitney test.

(L) Representative maximal h current traces in response to a 500-ms hyperpolarizing voltage step (-170 mV).

(M) Maximal dendritic h current at -170 mV was significantly decreased in (S)-ketamine-treated group compared with those from ACSF-treated group. **p < 0.01 by Mann-Whitney test.

(N) Steady-state I_h amplitude at different membrane potentials was significantly decreased in (S)-ketamine-treated group compared with those from ACSF-treated group. *p < 0.05 by two-way ANOVA with Sidark's multiple comparisons test. Traces in (A) and (E) were digitally filtered at 1 kHz for clarity. Data are expressed as mean ± SEM.

the normalized peak tail current ($I_{tail}/I_{tail\ max}$). At $\sim$270 μm from the soma, we observed that the $V_{1/2}$ of the h channel activation curve with (S)-ketamine treatment was significantly shifted to the left by around -12 mV (Figures 3I and 3J) ($V_{1/2}$ of ACSF: -108.2 mV versus $V_{1/2}$ of (S)-ket: -120.5 mV), whereas the slope factor was not different (Figures 3I and 3K) compared with those from ACSF-treated group. Furthermore, maximal dendritic I_h at -170 mV was significantly decreased in the (S)-ketamine-treated group compared with those from the ACSF-treated group (Figures 3L and 3M) (Max I_h of ACSF: -7.36 pA versus Max I_h of (S)-ket: -5.09 pA). In addition, steady-state I_h amplitude at different membrane potentials was significantly decreased in the (S)-ketamine-treated group compared with those from the ACSF-treated group (Figure 3N). Thus, both current-clamp measurements of I_h-sensitive properties (Figures 1 and 2) and direct recordings of I_h (Figure 3) indicate that the effects of (S)-ketamine occur in the dendrite but not in the soma in unstressed conditions. We then asked whether (S)-ketamine reduced I_h of dorsal CA1 neurons from the CUS model of depression.

(S)-Ketamine Reduced Somatic and Dendritic I_h-Related Properties in the CUS Model of Depression

Rats exposed to CUS for 2–3 weeks (Figure 4A) showed decreased locomotor activity (Figures 4B and 4C) and center square entries (Figures 4B and 4D) in the open field test and decreased sucrose preference (Figure 4E) in a two-bottle choice test, consistent with previous work (Kim et al., 2018). We then examined whether (S)-ketamine exerted rapid and sustained antidepressant effects in the CUS model of depression. Unstressed and CUS rats were split into four groups: (1) unstressed rats injected with saline 1 h before forced swim test (FST), (2) unstressed rats injected with (S)-ketamine (15 mg/kg intraperitoneal [i.p.] injection) 1 h before FST, (3) CUS rats injected with saline 24 h before FST, and (4) CUS rats injected with (S)-ketamine (15 mg/kg i.p. injection) 24 h before FST. CUS-exposed rats displayed an increase in passive activity (i.e., behavioral despair) that was reversed 1 h (Figures 4F) and 24 h (Figure 4G) after (S)-ketamine treatment in the FST, indicating the rapid and sustained antidepressant effects of (S)-ketamine. After the behavioral tests, acute dorsal hippocampal slices from saline-treated unstressed or CUS rats were prepared. Consistent with previous work (Kim et al., 2018), dorsal CA1 neurons from CUS-treated rats showed decreased somatic R_{in} and increased somatic f_R (Figure S7A) at different membrane potentials compared with those from the unstressed rats. Given that chronic stress has been shown to produce hypoactive neuronal excitability of dorsal CA1 neurons (Kim et al., 2018), we tested whether there was a change in neuronal excitability in the CUS model of depression. The number of action potential (APs) at the RMP in response to depolarizing current steps (30–400 pA for 750 ms) was significantly decreased in dorsal CA1 neurons from CUS-treated group compared with those from the unstressed group (Figure S7B).

We previously reported that the expression of the HCN1 subunit of HCN channels and I_h were upregulated in the soma, but not in the dendrite of dorsal CA1 neurons following CUS (Kim et al., 2018). Given that (S)-ketamine reduced dendritic but not somatic recordings consistent with the influence of I_h on dorsal CA1 neurons in unstressed conditions (Figure 1), we next examined whether (S)-ketamine reduced somatic and/or dendritic I_h-sensitive properties in the CUS model of depression. R_{in} and f_R at different membrane potentials were determined using whole-cell current-clamp recordings at the soma (Figures 5A–5C) and dendrite (Figures 5D–5F). Consistent with the results shown in Figure 1, (S)-ketamine did not affect somatic I_h-sensitive measurements in unstressed rats (Figure 5B). However, (S)-ketamine reduced the CUS-induced upregulation of somatic I_h-sensitive measurements (i.e., increased R_{in} and decreased f_R) at depolarized membrane potentials (Figure 5C). Dendritic I_h-sensitive measurements were significantly reduced at depolarized membrane potentials in both unstressed (Figure 5E) and CUS (Figure 5F) groups. Consistent with the effect of (S)-ketamine on somatic R_{in}, the number of APs elicited by depolarizing current steps was increased by (S)-ketamine in post-CUS but not unstressed CA1 neurons (Figures 5G–5J).
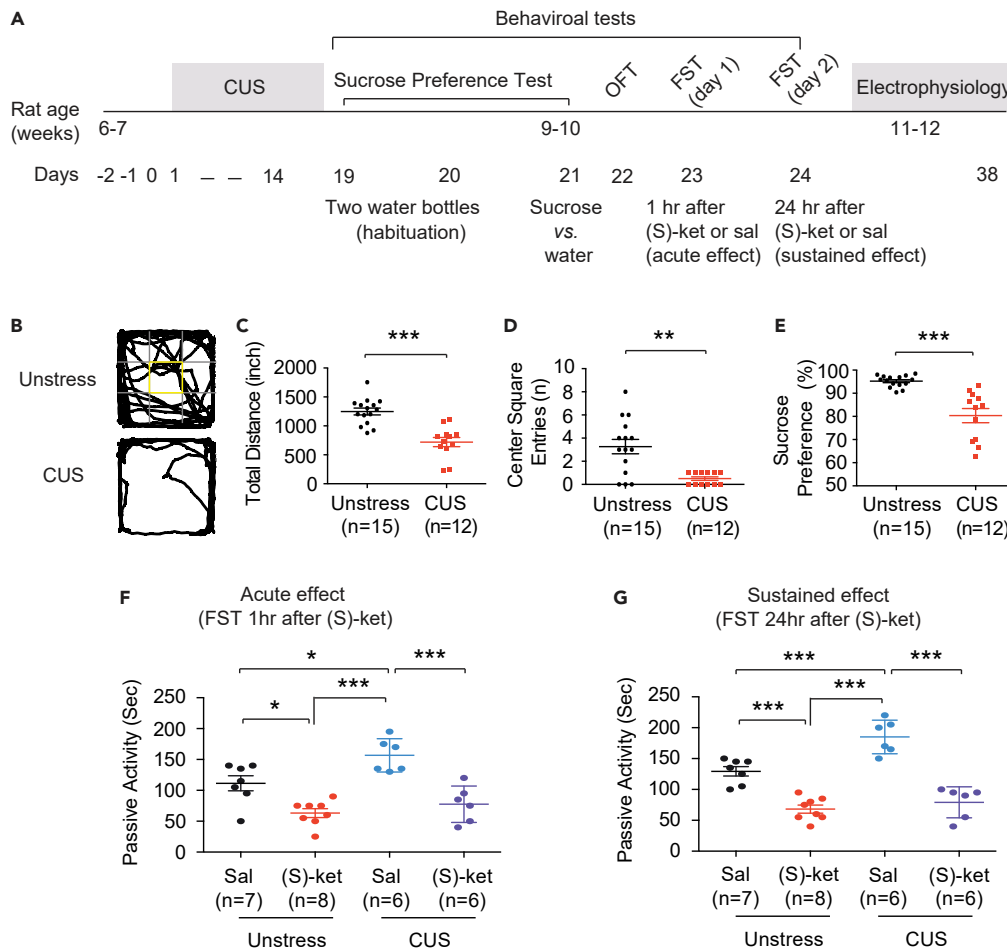
Figure 4. Rapid and Sustained Antidepressant-like Effects of (S)-Ketamine in the CUS Model of Depression

(A) Timeline of CUS, behavioral tests, and electrophysiology.

(B–D) (B) Representative video tracking images during the last 5 min of open field test of age-matched individual rats—unstressed versus CUS groups. CUS-treated rats showed decreases in total distance (C) and center square entries (D) compared with those from unstressed group. **p < 0.01 and ***p < 0.001 by Mann-Whitney test.

(E) CUS-treated rats showed decreased sucrose preference. ***p < 0.001 by Mann-Whitney test.

(F) Passive activity was significantly decreased 1 h after (S)-ketamine treatment (15 mg/kg, i.p. injection) in either unstressed or CUS groups (i.e., acute effects). *p < 0.05 and ***p < 0.001 by one-way ANOVA with Tukey multiple comparisons test.

(G) Passive activity was significantly decreased 24 h after (S)-ketamine treatment in either unstressed or CUS groups (i.e., sustained effects). ***p < 0.001 by one-way ANOVA with Tukey multiple comparisons test. Data are expressed as mean ± SEM.

Because the (S)-ketamine-induced reduction in dendritic I_h-sensitive properties was independent of barium-sensitive conductances and cAMP-dependent signaling in unstressed conditions (Figure 2), we next examined whether the same was true for the somatic effects observed following CUS. V_m, R_{in}, and f_R were monitored during baseline, application of 25 μM Ba^{2+}, and addition of 50 μM (S)-ketamine application (with 25 μM Ba^{2+}) in dorsal CA1 neurons (Figure S8). 25 μM Ba^{2+} significantly depolarized the membrane potential (Figure S9A) and increased R_{in} (Figure S9B), with no change in f_R (Figure S9C) in dorsal CA1 neurons of both unstressed and CUS groups. Somatic I_h-sensitive measurements (i.e., R_{in} and f_R) were not altered at different membrane potentials in the presence of Ba^{2+} following (S)-ketamine application in the dorsal CA1 neurons of unstressed group (Figures 5K, S9D, and S9E). On the other hand, the CUS-induced upregulation of somatic I_h-sensitive measurements was significantly changed at depolarized membrane potentials in the presence of Ba^{2+} following (S)-ketamine application in the dorsal CA1 neurons of CUS group (Figures 5L, S9F, and S9G). We next examined whether the effect of (S)-ketamine on CUS-induced
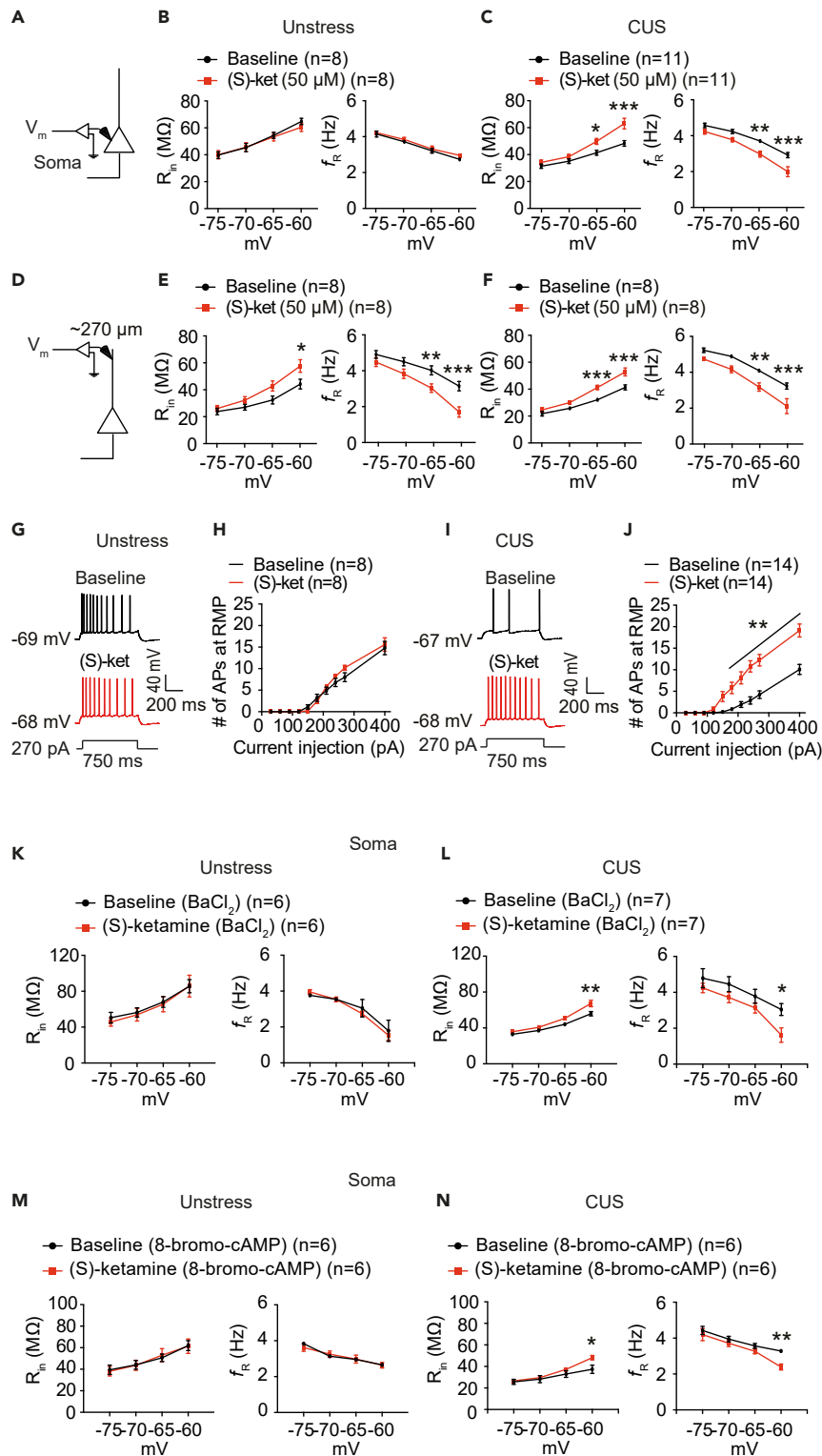
Figure 5. (S)-Ketamine Altered Somatic and Dendritic I_h-Sensitive Measures in the Dorsal CA1 Neurons of CUS Group

(A and D) Schematic of the somato-apical trunk depicting the somatic (A) and the dendritic (D) recordings.

(B) Somatic R_{in} and f_R at different membrane potentials were not changed following (S)-ketamine application in unstressed group.

(C) (S)-ketamine increased somatic R_{in} and decreased f_R at depolarized membrane potentials in CUS group. $*p < 0.05$, $**p < 0.01$, $***p < 0.001$ by two-way ANOVA with Sidark's multiple comparisons test.

(E and F) Dendritic R_{in} and f_R at depolarized membrane potentials were significantly changed following (S)-ketamine application in unstressed (E) and CUS (F) groups. $*p < 0.05$, $**p < 0.01$, $***p < 0.001$ by two-way ANOVA with Sidark's multiple comparisons test.

(G and I) Representative voltage responses at RMP with somatically injecting (270 pA; 750 ms) depolarizing current before (black) and after (red) (S)-ketamine treatment.

(H) The number of action potentials was not changed following (S)-ketamine application in dorsal CA1 neurons of unstressed group.

(J) A CUS-induced reduction of neuronal excitability was significantly increased following (S)-ketamine application in the dorsal CA1 neurons. $**p < 0.01$ by two-way ANOVA with Sidark's multiple comparisons test.

(K and M) In unstressed group, somatic R_{in} and f_R were not significantly altered at different membrane potentials in the presence of barium chloride (K, 25 μM) or 8-bromo-cAMP (M, 100 μM) following (S)-ketamine application.

(L and N) In CUS group, CUS-induced upregulation of somatic I_h-sensitive measurements were significantly changed at depolarized membrane potentials in the presence of barium chloride (L, 25 μM) or 8-bromo-cAMP (N, 100 μM) following (S)-ketamine application. $*p < 0.05$, $**p < 0.01$ by two-way ANOVA with Sidark's multiple comparisons test. Data are expressed as mean $\pm$ SEM.

somatic I_h was affected by 8-bromo-cAMP treatment (100 μM) in the dorsal CA1 neurons of CUS group. V_m, R_{in}, and f_R were monitored during baseline (100 μM 8-bromo-cAMP) and addition of 50 μM (S)-ketamine application (with 100 μM 8-bromo-cAMP) in the dorsal CA1 neurons (Figure S10). In the unstressed group, somatic I_h-sensitive measurements were not changed at different membrane potentials in the presence of 8-bromo-cAMP following (S)-ketamine application (Figures 5M, S11A, and S11B). However, CUS-induced somatic I_h-sensitive measurements were significantly changed at depolarized membrane potentials in the presence of 8-bromo-cAMP following (S)-ketamine application (Figures 5N, S11C, and S11D). These results suggest that the effects of (S)-ketamine on the CUS-induced upregulation of somatic I_h were independent of barium-sensitive conductances and cAMP-dependent signaling.

Direct Measurements Showed that (S)-Ketamine Reduced Somatic and Dendritic I_h in the CUS Model of Depression

We next examined the somatic effect of (S)-ketamine on voltage-dependent gating of h channel and the amplitude of h current in the CUS model of depression. We performed cell-attached patch-clamp recordings from the CUS-soma of dorsal CA1 neurons in the presence of D-AP5 and DNQX with or without (S)-ketamine treatment (50 μM, 30 min). Consistent with the results showing decreased somatic R_{in}, increased somatic f_R, and decreased in the number of APs in the dorsal CA1 neurons of the CUS group, we found that the $V_{1/2}$ of the h channel activation curve for CUS group was significantly shifted to the right by around +29 mV ($V_{1/2}$ of unstress-ACSF: −116.8 mV versus $V_{1/2}$ of CUS-ACSF: −88 mV), whereas the slope factor was not different compared with those from the unstressed group (Figures 6A–6C). Maximal somatic I_h at −170 mV was significantly increased in the dorsal CA1 neurons of the CUS group compared with those from unstressed group (Figures 6D and 6E) (Max I_h of unstress-ACSF: −0.59 pA versus Max I_h of CUS-ACSF: −3.89 pA). Steady-state I_h amplitude at different membrane potentials was significantly higher for CUS group than those from unstressed group (Figure 6F). Thus, the CUS-induced decrease in R_{in} and increase in f_R was mediated by an increased h current and a depolarizing shift to the h channel activation curve. When CUS-dorsal CA1 neurons were treated with (S)-ketamine (50 μM, 30 min), the $V_{1/2}$ of the h channel activation curve was significantly shifted to the left by around −23 mV (Figures 7A–7C) ($V_{1/2}$ of ACSF: −88 mV versus $V_{1/2}$ of (S)-ket: −110.9 mV), whereas the slope factor was not different (Figures 7A, 7B, and 7D) compared with those from the ACSF-treated CUS group. The CUS-induced increase in maximal somatic I_h was significantly decreased in the dorsal CA1 neurons of the (S)-ketamine-treated CUS group compared with those from the ACSF-treated CUS group (Figures 7E and 7F) (Max I_h of CUS-ACSF: −3.89 pA versus Max I_h of CUS-(S)-ketamine: −1.5 pA). Furthermore, steady-state I_h amplitude at different membrane potentials was significantly decreased in (S)-ketamine-treated group compared with those from ACSF-treated group (Figure 7G). Therefore, (S)-ketamine-induced reduction of somatic I_h was mediated by changes in the activation properties of the channels in the CUS model of depression.
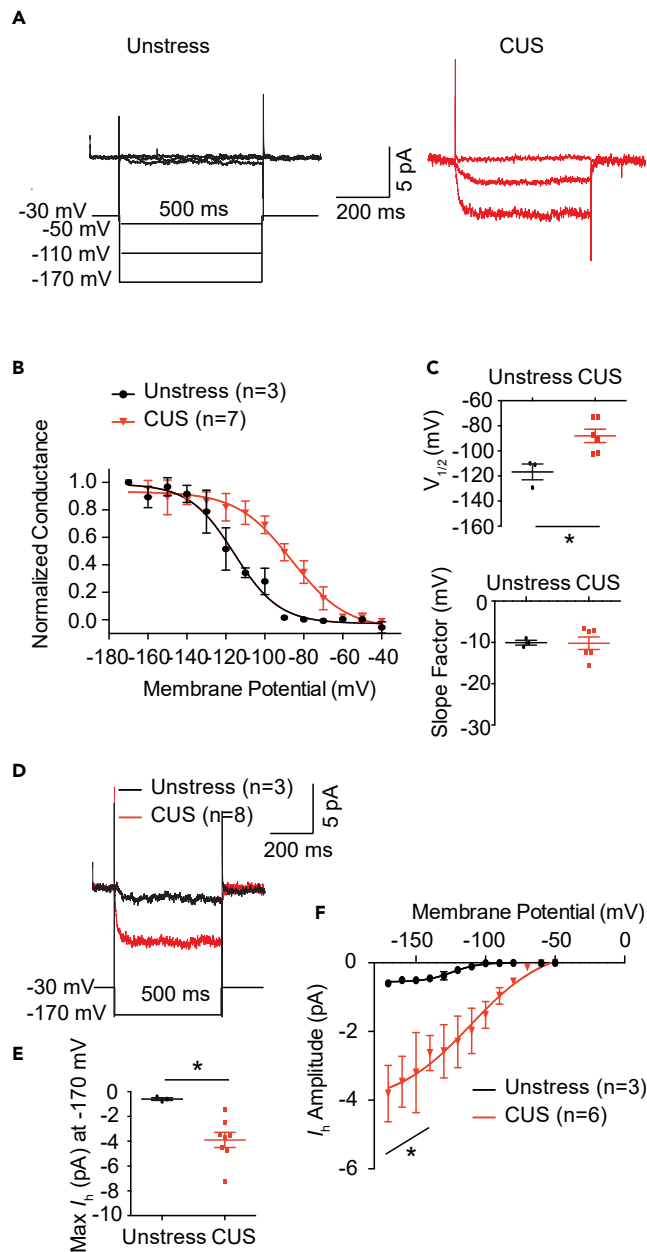
Figure 6. Changes in Voltage-Dependent Gating of *h* Channel and the Amplitude of *h* Current of Dorsal CA1 Neurons in the CUS Model of Depression

(A) Somatic *h* current was measured from unstressed group and CUS group of dorsal CA1 neurons with 500-ms hyperpolarizing voltage steps ranging from −40 mV to −170 mV in −10-mV increments from a holding potential of −30 mV.

(B) The voltage dependence of activation for *h* channel was determined from the somatic steady-state gV (ss gV) relationship. The activation curve was fitted a Boltzmann function with the following values: unstressed group $V_{1/2}$ = −116.8 mV, k = −10.07 mV; CUS group $V_{1/2}$ = −88.07 mV, k = −10.2 mV.

(C) The half-activation voltage ($V_{1/2}$) was significantly shifted to the right by +29 mV, whereas the slope factor was not different compared with those from unstressed group. *$p < 0.05$ by Mann-Whitney test.

(D) Representative maximum *h* current traces in response to a 500-ms hyperpolarizing voltage step (−170 mV).

(E) Maximal somatic *h* current at −170 mV was significantly higher for CUS group than those of unstressed group. *$p < 0.05$ by Mann-Whitney test.

Figure 6. Continued

(F) Steady-state I_h amplitude at different membrane potentials was significantly higher for CUS group than those for unstressed group. *p < 0.05 by two-way ANOVA with Sidark's multiple comparisons test. Traces in (A) and (D) were digitally filtered at 1 kHz for clarity. Data are expressed as mean ± SEM.

(S)-Ketamine Pretreatment Provided Resiliency to CUS

We have previously shown that lentiviral-mediated reduction of HCN1 subunit of HCN channels in the dorsal CA1 region before exposure to CUS provides resiliency to CUS (Kim et al., 2018). Therefore, we next investigated whether (S)-ketamine pretreatment before the onset of the CUS-induced depression prevented the CUS-dependent behavioral phenotypes and neuropathological changes. Unstressed and CUS rats were split into two groups, respectively, (1) saline-pretreated unstressed group, (2) (S)-ketamine-pretreated unstressed group, (3) saline-pretreated CUS group, and (4) (S)-ketamine-pretreated CUS group. Rats were administered a single injection of saline or (S)-ketamine (15 mg/kg, i.p. injection) 7 days before the onset of CUS (Figure 8A). After 2–3 weeks of CUS, we performed a series of behavioral tests such as sucrose preference test, open field test, and FST. In the unstressed group, there were no significant differences in locomotor activity and center square entries between saline- and (S)-ketamine-pretreated groups in the open field test (Figures 8B–8D). Saline-pretreated CUS rats showed decreased locomotor activity and center square entries compared with those from unstressed group (either saline- or (S)-ketamine-pretreated) (Figures 8B–8D), indicating anxiogenic-like behaviors. Interestingly, (S)-ketamine pretreatment in the CUS group prevented CUS-induced decreases in locomotor activity and center square entries compared with those from the saline-pretreated CUS group (Figures 8B–8D), suggesting the prevention of the CUS-induced anxiogenic-like behaviors by (S)-ketamine. Saline-pretreated CUS rats showed decreased sucrose preference (Figure 8E) and increased passive activity (Figure 8F) compared with those from unstressed group (saline- or (S)-ketamine-pretreated) or (S)-ketamine-pretreated CUS group, indicating the CUS-induced anhedonia and behavioral despair. On the other hand, (S)-ketamine pretreatment in the CUS group prevented decreased sucrose preference (Figure 7E) and increased passive activity time (Figure 8F) compared with those from the saline-pretreated CUS group, suggesting the prevention of the CUS-induced anhedonia and behavioral despair by (S)-ketamine.

Following the behavioral tests, whole-cell current-clamp recordings were made from the soma and dendrite. Somatic R_{in} and f_R at RMP (Figures 9A–9C) and at different membrane potentials (Figure 9D) were not significantly different between saline- and (S)-ketamine-pretreated unstressed groups. Dorsal CA1 neurons from the saline-pretreated CUS group had a lower R_{in} and a higher f_R at RMP (Figures 9B and 9C) and at different membrane potentials (Figures S12A and S12B) compared with those from either the unstressed group (saline- or (S)-ketamine-pretreated) or (S)-ketamine-pretreated CUS group. Interestingly, (S)-ketamine pretreatment in CUS group prevented the CUS-induced upregulation of somatic I_h-sensitive measurements at RMP (Figures 9B and 9C) and at different membrane potentials (Figure 9E). Consistent with a previous work (Kim et al., 2018), there were no significant differences in dendritic I_h-sensitive measurements between groups (Figure S13). These results suggest that (S)-ketamine pretreatment before the onset of depression prevented the CUS-induced upregulation of somatic I_h.

(S)-Ketamine Pretreatment Prevented the CUS-Induced Neuropathological Changes

Functional neuroimaging of patients with major depression shows bimodal, abnormal regional metabolic activities in limbic-cortical areas, including hippocampus, which can be reversed by clinical antidepressant treatment or chronic electrical stimulation (Mayberg et al., 2000, 2005). Similar observations have been reported in chronic stress-induced animal models of depression, which show increased neuronal excitability of lateral amygdala neurons (Rosenkranz et al., 2010) and decreased neuronal excitability of dorsal CA1 neurons (Kim et al., 2018). We, therefore, examined whether (S)-ketamine pretreatment before the onset of the CUS-induced depression prevented the CUS-induced neuropathological changes (i.e., upregulation of somatic I_h and reduced neuronal excitability). There were no significant differences in the number of APs measured in the dorsal CA1 neurons between the saline-pretreated and (S)-ketamine-pretreated unstressed groups (Figures 10A and 10B). However, we consistently observed decreased neuronal excitability in the saline-pretreated CUS group compared with those from the saline-pretreated unstressed group (Figure S14). A CUS-induced decrease in neuronal excitability was normalized in the dorsal CA1 neurons of (S)-
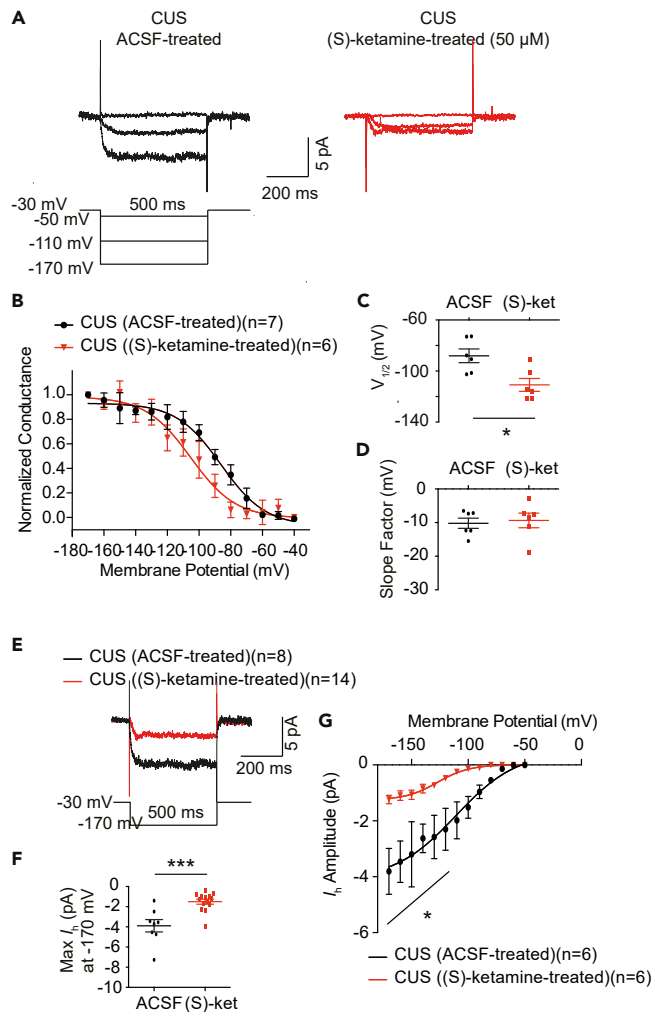
Figure 7. (S)-Ketamine Changed Voltage-Dependent Gating of *h* Channel and the Amplitude of *h* Current in the CUS Model of Depression

(A) Somatic *h* current was measured with cell-attached patches from ACSF-treated or (S)-ketamine-treated (30 min) dorsal CA1 neurons with 500-ms hyperpolarizing voltage steps ranging from −40 mV to −170 mV in −10-mV increments from a holding potential of −30 mV.

(B) The voltage dependence of activation for *h* channel was determined from the somatic steady-state GV relationship. The activation curve was fitted with a Boltzmann function with the following values: ACSF treatment $V_{1/2}$ = −88.07 mV, k = −10.2 mV, (S)-ketamine treatment $V_{1/2}$ = −110.9 mV, k = −9.36 mV.

(C and D) (C) The half-activation voltage of *h* channel ($V_{1/2}$) with (S)-ketamine treatment was significantly shifted to the left by around −23 mV, whereas the slope factor (D) was not different compared with those from ACSF-treated group. *p < 0.05 by Mann-Whitney test.

(E) Representative maximal *h* current traces in response to a 500-ms hyperpolarizing voltage step (−170 mV).

(F) Maximal somatic *h* current at −170 mV was significantly different between ACSF-treated and (S)-ketamine-treated CUS groups.

(G) I-V curve was significantly altered in (S)-ketamine-treated group compared with those from ACSF-treated group. Traces in (A) and (E) were digitally filtered at 1 kHz for clarity. *p < 0.05 by two-way ANOVA with Sidark's multiple comparisons test. Data are expressed as mean ± SEM.

ketamine-pretreated CUS group (Figures 10A and 10C). There were no significant differences in AP properties at RMP such as amplitude, peak, half-width, max dv/dt, and threshold (Figure S15). These results suggest that (S)-ketamine pretreatment before the onset of depression is sufficient to prevent the CUS-induced neuropathological changes such as the upregulation of I_h-sensitive measures and decrease in neuronal excitability.
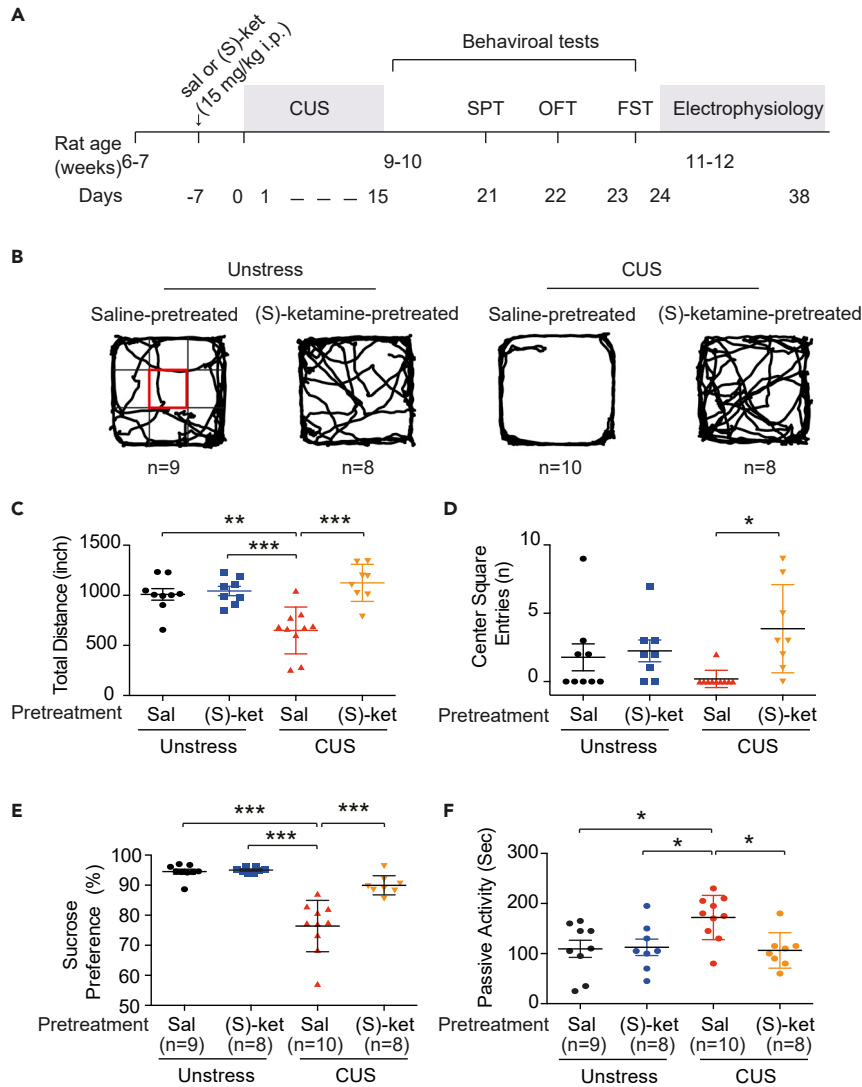
Figure 8. (S)-Ketamine Pretreatment Provided Resiliency to CUS

(A) Timeline of CUS, behavioral tests, and electrophysiology.

(B) Representative video tracking images during the last 5 min of open field test of age-matched individual rats—unstressed (sal- or (S)-ket-pretreated) versus CUS (sal- or (S)-ket-pretreated) rats.

(C and D) (S)-ketamine-pretreated CUS rats showed increases in total distance (C) and center square entries (D) compared with those from unstressed (sal- or (S)-ket-pretreated) or saline-pretreated CUS group. *p < 0.05, **p < 0.01, ***p < 0.001 by one-way ANOVA with Tukey multiple comparisons test.

(E and F) (S)-ketamine-pretreated CUS rats showed increased sucrose preference (E) and decreased passive activity time (F) compared with those from unstressed (sal- or (S)-ket-pretreated) or saline-pretreated CUS group. *p < 0.05, ***p < 0.001 by one-way ANOVA with Tukey multiple comparisons test. Data are expressed as mean ± SEM.

Thapsigargin-Induced Anxiogenic- and Anhedonic-like Behaviors Were Reversed by (S)-Ketamine in the Dorsal CA1 Region

We previously reported that *in vivo* block of the SERCA pumps in CA1 region leads to anxiogenic-like behaviors in the open field test and upregulation of functional I_h, similar to that observed in rats following CUS (Kim et al., 2018). To test whether (S)-ketamine's antidepressant effects are via the I_h/HCN1 channels, we performed *in vivo* infusion of TG, an irreversible inhibitor of the SERCA pumps, followed by infusion of (S)-ketamine. The specific doses of D-AP5 (25 μM) and (S)-ketamine (50 μM) used in *in vivo* study were chosen based on the results from *in vitro* experiments. To reduce the contribution of NMDA receptor
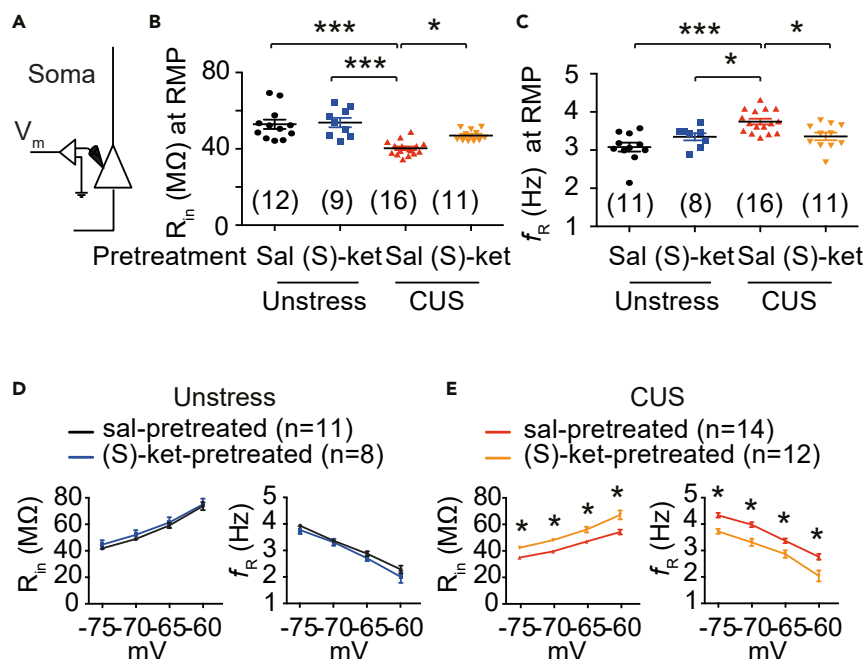
Figure 9. (S)-Ketamine Pretreatment Altered CUS-Induced Upregulation of Somatic I_h-Sensitive Measures

(A) Schematic of the somato-apical trunk depicting the somatic recordings.

(B and C) Dorsal CA1 neurons of (S)-ketamine-pretreated CUS group showed increased R_{in} (B) and decreased f_R (C) at RMP compared with those from saline-pretreated CUS group. *$p < 0.05$, ***$p < 0.001$ by one-way ANOVA with Tukey multiple comparisons test.

(D) There were no different somatic R_{in} and f_R between saline- and (S)-ketamine-pretreated unstressed groups at different membrane potentials (ranging from −60 to −75 mV, interval: −5 mV).

(E) Dorsal CA1 neurons of (S)-ketamine-pretreated CUS group showed increased R_{in} and decreased f_R at different membrane potentials compared with those from saline-pretreated CUS group. *$p < 0.05$ by two-way ANOVA with Sidark's multiple comparisons test. Data are expressed as mean ± SEM.

in behavioral tests, TG (1 μM) or (S)-ketamine (50 μM) was dissolved with D-AP5 (25 μM). Rats were bilaterally cannulated into the dorsal CA1 region (Figures 11C) and were housed individually. After a minimum 5-day recovery period, rats were divided into five groups: (1) saline, (2) D-AP5, (3) (S)-ketamine (with D-AP5), (4) TG (with D-AP5), and (5) TG (with D-AP5) followed by (S)-ketamine (with D-AP5) (Figures 11A). It has been reported that 10 μM D-AP5, a competitive NMDA receptor antagonist, is sufficient to block NMDA receptor-mediated currents (Benveniste and Mayer, 1991). Behaviorally, NMDA receptor dysfunction by intrahippocampal infusion of cerebrospinal fluid from anti-NMDA receptor encephalitis shows no changes in locomotor activity or anxiety-related behavior (Kersten et al., 2019). Consistently, rats bilaterally infused with 25 μM D-AP5 showed no changes in locomotor activity or anxiety level (Figures 11B–11E) compared with those from the saline-infused group. Consistent with a previous result (Kim et al., 2018), rats bilaterally infused with 1 μM TG (with D-AP5) showed decreased locomotor activity (Figures 11B and 11D) and center square entries (Figures 11B and 11E) indicating anxiogenic-like behavior compared with those from saline-infused group. Rats bilaterally infused with 50 μM (S)-ketamine (with D-AP5) showed increased center square entries (Figures 11B and 11E) indicating anxiolytic-like behavior compared with those from D-AP5 (25 μM)-infused group. Interestingly, 1 μM TG (with D-AP5) followed by 50 μM (S)-ketamine (with D-AP5) in the dorsal CA1 region increased center square entries compared with those from the TG-infused group, suggesting that TG-induced anxiogenic-like behavior was reversed by (S)-ketamine. Because cannulated rats were not suitable for an FST, we performed a sucrose preference test following the open field test (Figures 11F and 11G). TG-infused rats showed decreased sucrose preference during 13-h dark cycle compared with those from saline- or D-AP5- or (S)-ketamine-infused group (Figures 11G) without a change in total fluid intake (Figures 11F), indicating anhedonic-like behavior. Surprisingly, rats infused with TG followed by (S)-ketamine showed increased sucrose preference compared with those from TG-infused group (Figure 11G), indicating antidepressant-like effect of (S)-ketamine.
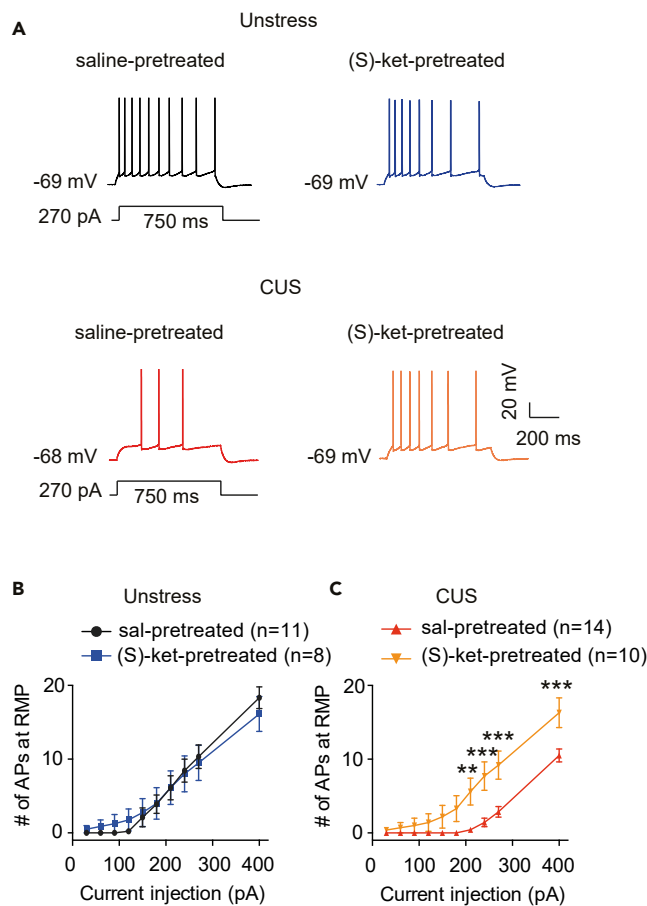
Figure 10. (S)-Ketamine Pretreatment Prevented the CUS-Induced Decrease in Neuronal Excitability
(A) Representative voltage responses with depolarizing current step (270 pA; 750 ms) at RMP.
(B) The number of action potentials was not different between saline- and (S)-ketamine-pretreated unstressed groups.
(C) Dorsal CA1 neurons of (S)-ketamine-pretreated CUS group showed increased action potential firing at RMP. **$p <$ 0.01, ***$p <$ 0.001 by two-way ANOVA with Sidark's multiple comparisons test. Data are expressed as mean $\pm$ SEM.

Thapsigargin-Induced Upregulation of Functional I_h Was Reversed by (S)-Ketamine in the Dorsal CA1 Region

Given that *in vivo* block of the SERCA pumps in dorsal CA1 region/neurons produces an anxiogenic-like behavior and upregulation of functional I_h (Kim et al., 2018), we hypothesized that *in vivo* infusion of TG followed by infusion of (S)-ketamine might alter functional I_h. Dorsal hippocampal slices were prepared immediately after a 10-min open field test (Figure 12A). Functional I_h (e.g., RMP, R_{in}, f_R, and # of APs) was determined using whole-cell current-clamp recordings at the soma in the presence of glutamatergic synaptic blockers (i.e., D-AP5 and DNQX). There were no differences in somatic RMP between groups (Figures S16A and S16C). Functional I_h at RMP was decreased (i.e., increased R_{in} and decreased f_R) in the dorsal CA1 neurons of the (S)-ketamine-infused group, whereas increased (i.e., decreased R_{in} and increased f_R) in the dorsal CA1 neurons of TG-infused group compared with those from the saline- or D-AP5-infused group (Figures S16A–S16E). TG-induced upregulation of functional I_h at RMP was decreased in the dorsal CA1 neurons of TG+(S)-ketamine group (Figures S16A–S16E). Dorsal CA1 neurons of (S)-ketamine-infused group showed significantly increased R_{in} (Figure 12B) and decreased f_R (Figure 12C) at different membrane potentials (ranging from −65 mV to −75 mV, interval −5 mV) compared with those from either saline- or D-AP5-infused group, indicating a decrease in functional I_h. Consistent with a previous result (Kim et al., 2018), dorsal CA1 neurons of TG-infused group showed decreased R_{in} (Figure 12B) and increased f_R (Figure 12C) at different membrane potentials compared with those from either saline- or D-AP5-infused group, indicating upregulation of functional I_h. Interestingly, dorsal CA1 neurons of TG+(S)-ketamine group showed increased R_{in} (Figure 12B) and decreased f_R (Figure 12C) at different membrane potentials
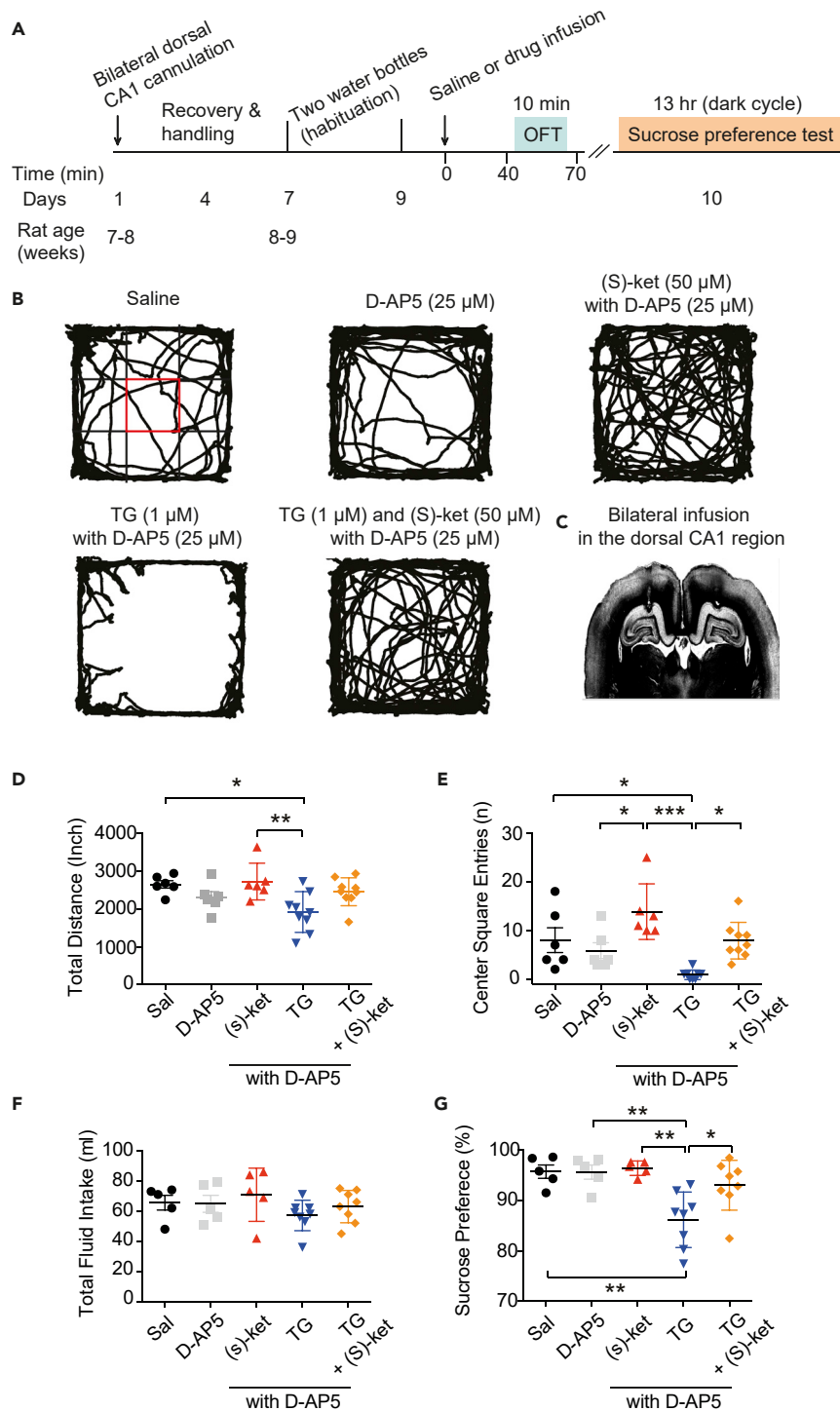
Figure 11. Thapsigargin-Induced Anxiogenic- and Anhedonic-like Behaviors Were Reversed by (S)-Ketamine

(A) Timeline of thapsigargin and (S)-ketamine experiment.

(B) Representative video tracking during the 10 min of open field test of age-matched individual rats with saline, D-AP5 (25 μM), (S)-ketamine (50 μM) with D-AP5 (25 μM), thapsigargin (1 μM) with D-AP5 (25 μM), or infusion of thapsigargin (with D-AP5) followed by infusion of (S)-ketamine (with D-AP5).

(C) Representative coronal sections of the brains display the location of the infusion needle track within the dorsal hippocampus of CA1.

Figure 11. *Continued*

(D) Total distance during a 10-min open field test. *In vivo* infusion of TG decreased locomotor activity. $*p < 0.05$, $**p < 0.01$ by one-way ANOVA with Tukey multiple comparisons test.

(E) (S)-ketamine increased center square entries, whereas TG decreased center square entries compared with those from either saline- or D-AP5-infused group. TG-induced anxiogenic-like behavior was reversed by (S)-ketamine. $*p < 0.05$, $***p < 0.001$ by one-way ANOVA with Tukey multiple comparisons test.

(F) There were no significant differences in total fluid intake between groups.

(G) TG-injected rats showed decreased sucrose preference compared with those from saline- or D-AP5- or (S)-ketamine-infused group. TG-induced anhedonic-like behavior was reversed by (S)-ketamine.

$*p < 0.05$, $**p < 0.01$ by one-way ANOVA with Tukey multiple comparisons test. Data are expressed as mean $\pm$ SEM.

compared with those from TG-infused group indicating the reversal of the effects of TG by (S)-ketamine. The number of AP firings elicited by depolarizing current steps was significantly increased in the dorsal CA1 neurons of (S)-ketamine-infused group compared with those from either saline- or D-AP5-infused group (Figures 12D and 12E) indicating an increase in neuronal excitability. Consistent with TG-induced decrease in R_{in}, the number of APs was significantly decreased in the dorsal CA1 neurons of TG-infused group compared with those from either saline- or D-AP5-infused group (Figures 12D and 12E) indicating a decrease in neuronal excitability. Dorsal CA1 neurons of TG+(S)-ketamine group showed increased neuronal excitability compared with those from the TG-infused group (Figures 12D and 12E), suggesting that TG-induced hypoexcitability was reversed by (S)-ketamine.

DISCUSSION

We found that (S)-ketamine reduced dendritic I_h in unstressed conditions, whereas it decreased both somatic and dendritic I_h in the CUS model of depression. The (S)-ketamine-induced change in I_h-sensitive parameters was consistent with the reduction in h current and a hyperpolarizing shift to the h channel activation curve. (S)-ketamine also reversed the CUS-induced decreases in neuronal excitability. (S)-ketamine pretreatment before the onset of depression prevented the CUS-induced abnormal behaviors (i.e., anxiogenic- and depressive-like behaviors) and neuropathological changes (i.e., upregulation of somatic I_h and a decrease in neuronal excitability). Finally, *in vivo* infusion of TG-induced anxiogenic- and anhedonic-like behaviors and upregulation of functional I_h were reversed by (S)-ketamine.

In humans a single sub-anesthetic dose of (R,S)-ketamine (0.5 mg/kg, i.v. injection for 40 min) has been shown to have rapid (hours) and sustained (days to a week) antidepressant effects in TRD (Berman et al., 2000; Zarate et al., 2006a). Recently, Canuso et al., reported efficacy and safety of FDA-approved intranasal (S)-ketamine in TRD and antisuicidal effects in major depression (Canuso et al., 2018). In addition, continued treatment with intranasal (S)-ketamine plus an oral antidepressant had a significantly delayed time to relapse (i.e., sustained effect) among patients with TRD compared with placebo nasal spray plus an oral antidepressant treatment for 16 weeks (Daly et al., 2019). In preclinical studies, a single sub-anesthetic dose of (R,S)-ketamine (10–15 mg/kg i.p.) produces rapid and sustained antidepressant-like effects in the FST (Autry et al., 2011; Li et al., 2010). Consistent with (R,S)-ketamine's antidepressant effects, we also observed that a single sub-anesthetic dose of (S)-ketamine (15 mg/kg i.p.) produced rapid (1 h after (S)-ket treatment) and sustained (24 h after (S)-ket treatment) antidepressant effects in the FST. In spite of the compelling clinical and preclinical evidence supporting (R,S)-ketamine's rapid and robust antidepressant effects on depression, the cellular mechanisms underlying its antidepressant actions are still under debate. Because (R,S)-ketamine is a noncompetitive NMDA receptor antagonist (Anis et al., 1983), the prevailing hypothesis for (R,S)-ketamine's antidepressant effects is through blockade of NMDA receptors. However, it has been reported that antidepressant-relevant concentrations of (2R,6R)-hydroxynorketamine (HNK; less than 10 µM), one of ketamine's metabolites, exert acute antidepressant-like effects in the social defeat model of depression in an NMDA receptor-independent manner (Zanos et al., 2016; Lumsden et al., 2019). In contrast, Suzuki et al., reported that 50 µM (R,S)-ketamine or (2R,6R)-HNK blocks synaptic NMDA receptors (Suzuki et al., 2017). Furthermore, rapid antidepressant effects of (R,S)-ketamine are mediated by the opioid receptor activation, although the sample size (n = 7) of (R,S)-ketamine-responsive patients with TRD is small (Williams et al., 2018). Despite the controversy over the role of NMDA receptors in the antidepressant action of (R,S)-ketamine (Preskorn et al., 2008; Lodge and Mercier, 2015; Zarate et al., 2006b; Zanos et al., 2016; Suzuki et al., 2017; Williams et al., 2018), the antidepressant effect is generally associated with increased BDNF/mTOR signaling, a decrease in eEF2 kinase, and synaptic AMPA receptors (Li et al., 2010; Autry et al., 2011; Maeng et al., 2008).
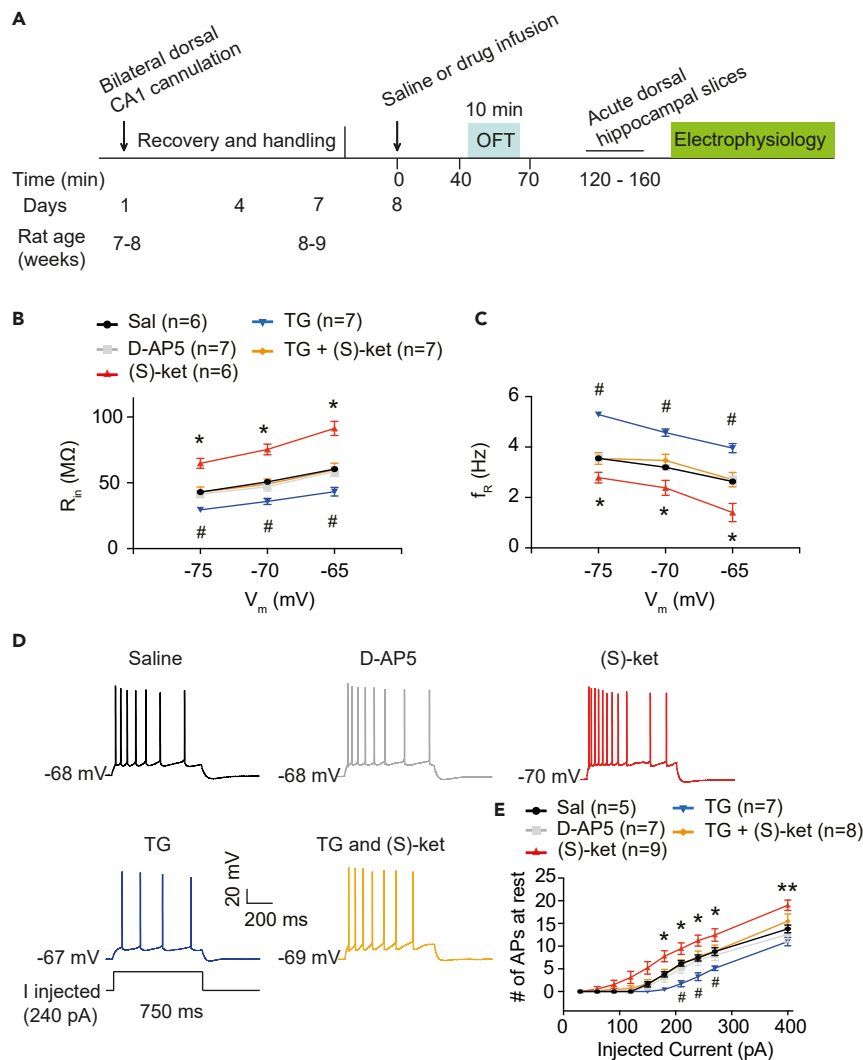
Figure 12. TG-Induced Upregulation of Functional I_h Was Reversed by (S)-Ketamine

(A) Timeline of thapsigargin and (S)-ketamine experiment.

(B and C) Dorsal CA1 neurons of (S)-ketamine-infused group showed increased R_{in} (B) and decreased f_R (C) at different membrane potentials (ranging from −65 mV to −75 mV; −5 mV interval) compared with those from saline- or D-AP5-infused group. Dorsal CA1 neurons of TG-infused group showed decreased R_{in} (B) and increased f_R (C) at different membrane potentials compared with those from saline- or D-AP5-infused group. Dorsal CA1 neurons of TG+(S)-ketamine-infused group showed that TG-induced upregulation of functional I_h was reversed by (S)-ketamine. *$p < 0.05$ (sal or D-AP5 versus (S)-ket) and #$p < 0.05$ (sal or D-AP5 versus TG) by two-way ANOVA with Sidark's multiple comparisons test.

(D) Representative voltage responses with depolarizing current step (240 pA; 750 ms) at RMP.

(E) Dorsal CA1 neurons of (S)-ketamine-infused group showed increased action potential firing at RMP, whereas decreased at RMP in the dorsal CA1 neurons of TG-infused group compared with those from saline- or D-AP5-infused group. Dorsal CA1 neurons of TG+(S)-ketamine-infused group showed increased neuronal excitability compared with those from TG-infused group. *$p < 0.05$, **$p < 0.01$ (sal or D-AP5 versus (S)-ket) and #$p < 0.05$ (sal or D-AP5 versus TG) by two-way ANOVA with Sidark's multiple comparisons test. Data are expressed as mean ± SEM.

We have previously reported that a lentiviral small hairpin RNA-mediated reduction of the HCN1 subunit of h-channels (and I_h) in the dorsal CA1 region/neurons leads to an increase in neuronal excitability, upregulation of BDNF/phosphorylation of mTOR protein expression, and an increase in excitatory synaptic transmission (i.e., field excitatory postsynaptic potential slope), which contributes to antidepressant- and anxiolytic-like behaviors in unstressed conditions (Kim et al., 2012). Given that a single sub-anesthetic dose of (R,S)-ketamine in the rodent produces similar downstream signaling pathways (e.g., increased

BDNF-mTOR signaling) and behavioral outcomes (antidepressant-like behaviors) (Li et al., 2010; Autry et al., 2011; Zanos et al., 2016), it is possible that (R,S)-ketamine-mediated antidepressant effects are associated with a reduction of I_h. Rats exposed to CUS for 2–3 weeks show anxiogenic-like (e.g., decreased locomotor activity and center square entries in the open field test) and depressive-like (e.g., decreased sucrose preference in a two-bottle choice test and increased passive activity in the FST) behaviors (Kim et al., 2018). Because CUS-treated rats showed decreased locomotor activity in the open field test, a correlation between locomotor activity and anxiety level is suggested. For example, a low dose of diazepam (1 mg/kg i.p.), an anxiolytic drug, increases locomotor activity and center square entries in the open field test, which can be interpreted as increased locomotion caused by decreased anxiety (Kim et al., 2012). Although CUS-treated rats showed increased anxiety, which might be caused by decreased exploration or increased innate fear response to a novel environment, there might be a limitation to this interpretation. In our previous report, somatic I_h and the expression of the HCN1 protein are upregulated in the dorsal CA1 neurons/region following CUS but not acute stress (Kim et al., 2018). This upregulation of somatic I_h is associated with chronic stress-induced elevated intracellular calcium levels (Narayanan et al., 2010; Kim et al., 2018). There is also a strong correlation between the time course of the increase in somatic I_h and the development of the depression-like symptoms (Kim et al., 2018). These results suggest a possible link between HCN channels and depression (Kim et al., 2018; Kim and Johnston, 2018). The important question was whether (S)-ketamine reduced the CUS-induced upregulation of I_h of dorsal CA1 neurons in the CUS model of depression.

Chen et al. reported that (S)-ketamine reduces HCN1 but not HCN2 subunit-mediated I_h via a hyperpolarizing shift in voltage dependence of activation in layer 5 cortical pyramidal neurons ($V_{1/2}$: ∼ −10 mV) and in HEK 293 cells expressing homomeric mouse HCN1 channels ($V_{1/2}$: ∼ −15 mV) with somatic recordings in unstressed conditions (Chen et al., 2009). We initially attempted to reproduce this (S)-ketamine reduction in somatic I_h-sensitive electrophysiological measurements (i.e., R_{in} and f_R) of dorsal CA1 neurons. However, we did not observe any changes in somatic I_h-sensitive measurements despite using four different concentrations of (S)-ketamine (20, 40, 80, 160 μM) in dorsal or ventral CA1 neurons with or without NMDA receptor blockers (Figure S2). Consistent with these negative results, we did not see any somatic changes in I_h-sensitive measurements following 50 μM (S)-ketamine in the presence of glutamatergic synaptic blockers (D-AP5 and DNQX). Given that HCN channels are heavily expressed in dendrites of CA1 neurons (Magee, 1998), we, therefore, measured I_h-sensitive measurements in dendrites in the presence of D-AP5 (25 or 50 μM) and DNQX. Indeed, (S)-ketamine reduced dendritic I_h-sensitive measurements (i.e., increased R_{in} and decreased f_R) at depolarized membrane potentials within 10–20 min. Consistent with this result, a reduction of I_h-sensitive measurements by (S)-ketamine was distance-dependent along the somatodendritic axis of dorsal CA1 neurons. Given a very low expression of HCN1 channels (therefore I_h) in the perisomatic region of dorsal CA1 neurons in unstressed conditions, it is possible that the lack of effects of (S)-ketamine on somatic I_h might be due to a very low expression of HCN1 channels at the soma and the difficulty of measuring I_h in cell-attached patches. It is also possible that heteromeric somatic h channel in unstressed conditions are composed predominantly of HCN2 subunits, which are insensitive to (S)-ketamine (Wang et al., 2001), but shift to predominantly HCN1-containing h channel after CUS. Further experiments will be needed to address these and other possibilities.

GIRK conductance in the dorsal CA1 neurons contributes to intrinsic membrane properties including R_{in} (Kim and Johnston, 2015). We found that the increased R_{in} by (S)-ketamine was independent of barium-sensitive conductances (GIRK and IRK) in both unstressed and CUS groups. HCN channels are also regulated by binding of cAMP to the cyclic nucleotide-binding domain, which results in a subunit specific generation of a depolarizing shift of the I_h voltage activation curve (Wang et al., 2001). Recently, Wray et al. showed that treatment of C6 glioma cells or primary astrocytes with (R,S)-ketamine (10 μM for 15 min) increases cAMP-dependent BDNF protein expression after 24 h (Wray et al., 2018). We, therefore, examined whether cAMP-dependent signaling was involved in the regulation of I_h by (S)-ketamine. 8-Bromo-cAMP is an activator of cAMP-dependent protein kinase. The (S)-ketamine-induced reduction in dendritic I_h in unstressed group or CUS-induced upregulation of somatic I_h was independent of cAMP-dependent signaling. We also examined the possibility that (S)-ketamine could further change I_h-sensitive measurements (e.g., R_{in}) after blockade of I_h by ZD7288. However, successive ZD7288 and (S)-ketamine wash-in experiment with dendrite recordings revealed that the ZD7288-induced change in R_{in} was not further altered by addition of (S)-ketamine treatment, suggesting an occlusion effect with (S)-ketamine.

Cell-attached patch-clamp recordings showed that (S)-ketamine treatment led to changes in voltage-dependence of h channel (i.e., a hyperpolarizing shift to the h channel activation curve) and the amplitude of h current (i.e., decreased maximal h current) in dendrites but not soma in the unstressed group. Consistent with previous results (Kim et al., 2018), somatic but not dendritic I_h-sensitive measurements of dorsal CA1 neurons were upregulated in the CUS model of depression. Cell-attached patch-clamp recordings at the soma revealed that the $V_{1/2}$ of the h channel activation curve for CUS group was significantly shifted to the right around +29 mV compared with those from unstressed group. Maximal I_h at −170 mV for CUS group was around − 3.89 pA, whereas maximal I_h for unstressed group was around −0.59 pA. Whole-cell current-clamp recordings revealed that (S)-ketamine significantly reduced the CUS-induced upregulation of somatic I_h-sensitive measurements of dorsal CA1 neurons at depolarized membrane potentials, whereas no changes in the unstressed group were observed. We also confirmed that (S)-ketamine treatment for CUS group led to a hyperpolarizing shift to the h channel activation curve around - 23 mV and a decrease in h current around −2.4 pA compared with those from ACSF-treated CUS group. (S)-ketamine also reduced dendritic I_h-sensitive measurements of dorsal CA1 neurons in both unstressed and CUS groups.

It has been reported that a single sub-anesthetic dose of (R,S)-ketamine pretreatment before the onset of stress prevents either chronic stress-induced depression-like behaviors (Brachman et al., 2016) or acute stress (e.g., inescapable tail shock)-induced fear responses or anxiety (Amat et al., 2016, Mcgowan et al., 2017). Consistent with these reports, we also observed that a single sub-anesthetic dose of (S)-ketamine pretreatment 1 week before the onset of CUS prevented the CUS-induced anxiogenic- and depressive-like behaviors. We have reported that a reduction of HCN1 protein expression in the dorsal CA1 region before the onset of CUS provides resiliency to the depression-like symptoms (Kim et al., 2018). In addition, knockdown of HCN1 protein expression or neuropeptide Y-induced reduction of I_h into basolateral amygdala is sufficient to exert resiliency to stress in rats (Silveira Villarroel et al., 2018). Interestingly, the saline-pretreated CUS group showed upregulation of somatic I_h, whereas no changes in the (S)-ketamine-pretreated CUS group were observed.

Functional neuroimaging of patients with major depression has shown bimodal, abnormal regional metabolic activities in different regions of limbic-cortical areas (Mayberg et al., 2000, 2005). Given a positive correlation between brain energy metabolism and neuronal excitability, abnormal change in neuronal excitability (e.g., a number of APs at RMP) has been reported following chronic stress (Kim et al., 2018; Rosenkranz et al., 2010). Dorsal CA1 neurons from CUS group had a lower R_{in} and a high f_R compared with those from unstressed group. As expected, neuronal excitability was significantly reduced in the dorsal CA1 neurons following CUS. This decrease in neuronal excitability was reversed by bath application of (S)-ketamine within 10–20 min. Furthermore, (S)-ketamine pretreatment before the onset of depression prevented CUS-induced decrease in neuronal excitability. Therefore, (S)-ketamine-induced changes in intrinsic membrane properties may contribute to the changes in behaviors (i.e., anxiolytic- and antidepressant-like behaviors).

Recently, Lumsden et al. reported that (2R,6R)-HNK, at the dose of 10 mg/kg (i.p), exerts antidepressant-like effects associated with increased mature BDNF and phosphorylation of mTOR protein expression (Lumsden et al., 2019). This antidepressant-relevant concentration of (2R,6R)-HNK (at dose of 10 mg/kg, i.p.) generates around 8 μM ketamine metabolite in the serum, whole brain, and ventral hippocampus (Lumsden et al., 2019). Given that the antidepressant-relevant concentrations of (R,S)-ketamine are ranging from 3 to 30 mg/kg (i.p.) in rodent (Kim et al., 2012; Lumsden et al., 2019; Autry et al., 2011; Iijima et al., 2012; Koike et al., 2013), their concentrations in the brain might be higher than estimated (e.g., more than 10 μM of (R,S)-ketamine and its metabolite). Similarly, Fava et al., reported that even higher concentration of (R,S)-ketamine (i.e., 1 mg/kg i.v. for 40 min) exerts antidepressant effects in TRD, whereas lower doses of (R,S)-ketamine (0.1 and 0.2 mg/kg i.v. for 40 min) do not exert clinically meaningful antidepressant effects (Fava et al., 2018). Consistent with dose-dependent effects of (R,S)-ketamine, we found that a reduction of dendritic I_h-sensitive measurements by (S)-ketamine was dose dependent in the dorsal CA1 neurons.

It has been reported that patients with depression showed an elevated basal intracellular Ca^{2+} concentration in platelets and lymphocytes (Kerr et al., 1992; Karst et al., 2000). In our previous reports (Narayanan et al., 2010; Kim et al., 2018), in vitro or in vivo block of the SERCA pumps in CA1 neurons increases perisomatic I_h. Furthermore, in vivo infusion of TG produces anxiogenic-like behavior, similar to that observed

in CUS model of depression (Kim et al., 2018). In this study, TG and (S)-ketamine were dissolved with D-AP5 to reduce the contribution of NMDA receptors in our *in vivo* study. We observed not only decreased center square entries in the open field test (i.e., anxiogenic-like behavior) but also decreased sucrose preference in the two-bottle choice test (i.e., anhedonic-like behavior) from *in vivo* TG-infused group. TG-induced changes in behaviors were reversed by (S)-ketamine. Whole-cell current-clamp recordings after a 10-min open field test revealed that dorsal CA1 neurons of (1) TG-infused group showed increased functional I_h (i.e., decreased R_{in} and increased f_R), (2) (S)-ketamine-infused group showed decreased functional I_h (i.e., increased R_{in} and decreased f_R), and (3) TG+(S)-ketamine-infused group showed decreased functional I_h. Consistent with changes in R_{in} from TG- or (S)-ketamine- or TG+(S)-ketamine-infused group, we observed similar changes in neuronal excitability from these groups. These behavioral and electrophysiological results suggest that (S)-ketamine's antidepressant effects are through a reduction of HCN1 channels, and therefore I_h, in the dorsal CA1 region/neurons.

In summary, we found that (S)-ketamine reduced dendritic but not somatic I_h in an NMDA receptor-independent manner in unstressed conditions. (S)-ketamine normalized the CUS-induced neuropathological changes, which resulted in reduced somatic I_h and increased neuronal excitability. A single dose of (S)-ketamine pretreatment before the onset of depression prevented the CUS-induced neuropathological changes. Finally, *in vivo* infusion of TG-induced anxiogenic- and anhedonic-like behaviors and upregulation of functional I_h were reversed by (S)-ketamine. To our knowledge, this is the first report that (1) (S)-ketamine reduced the CUS-induced upregulation of somatic I_h, (2) (S)-ketamine pretreatment before the onset of depression prevented the CUS-induced neuropathological changes such as upregulation of somatic I_h, and (3) antidepressant effects of (S)-ketamine are through a reduction of HCN1/I_h. Our findings suggest that the NMDA receptor-independent cellular mechanisms of (S)-ketamine reported here may underlie some of (S)-ketamine's antidepressant actions and resiliency to chronic stress.

Limitations of the Study

In this study, we systematically investigated the effects of (S)-ketamine on I_h. Further investigation is required, however, into whether a change in I_h by pretreatment of (S)-ketamine is due to direct or indirect effects on I_h. We only used male rats in this study.

Resource Availability

Lead Contact

Further information and requests for resources and reagents should be directed to and will be fulfilled by the Lead Contact, Chung Sub Kim (ckim5@augusta.edu).

Materials Availability

This study did not generate any new reagents.

Data and Code Availability

This published article includes all datasets/code generated or analyzed during this study.

METHODS

All methods can be found in the accompanying Transparent Methods supplemental file.

SUPPLEMENTAL INFORMATION

Supplemental Information can be found online at https://doi.org/10.1016/j.isci.2020.101239.

ACKNOWLEDGMENTS

REFERENCES

Amat, J., Dolzani, S.D., Tilden, S., Christianson, J.P., Kubala, K.H., Bartholomay, K., Sperr, K., Ciancio, N., Watkins, L.R., and Maier, S.F. (2016). Previous ketamine produces an enduring blockade of neurochemical and behavioral effects of uncontrollable stress. J. Neurosci. 36, 153–161.

Anis, N.A., Berry, S.C., Burton, N.R., and Lodge, D. (1983). The dissociative anaesthetics, ketamine and phencyclidine, selectively reduce excitation of central mammalian neurones by N-methyl-aspartate. Br. J. Pharmacol. 79, 565–575.

Autry, A.E., Adachi, M., Nosyreva, E., Na, E.S., Los, M.F., Cheng, P.F., Kavalali, E.T., and Monteggia, L.M. (2011). NMDA receptor blockade at rest triggers rapid behavioural antidepressant responses. Nature 475, 91–95.

Benveniste, M., and Mayer, M.L. (1991). Kinetic analysis of antagonist action at N-methyl-D-aspartic acid receptors. Two binding sites each for glutamate and glycine. Biophys. J. 59, 560–573.

Berman, R.M., Cappiello, A., Anand, A., Oren, D.A., Heninger, G.R., Charney, D.S., and Krystal, J.H. (2000). Antidepressant effects of ketamine in depressed patients. Biol. Psychiatry 47, 351–354.

Bostwick, J.M., and Pankratz, V.S. (2000). Affective disorders and suicide risk: a reexamination. Am. J. Psychiatry 157, 1925–1932.

Brachman, R.A., Mcgowan, J.C., Perusini, J.N., Lim, S.C., Pham, T.H., Faye, C., Gardier, A.M., Mendez-David, I., David, D.J., Hen, R., and Denny, C.A. (2016). Ketamine as a prophylactic against stress-induced depressive-like behavior. Biol. Psychiatry 79, 776–786.

Canuso, C.M., Singh, J.B., Fedgchin, M., Alphs, L., Lane, R., Lim, P., Pinter, C., Hough, D., Sanacora, G., Manji, H., and Drevets, W.C. (2018). Efficacy and safety of intranasal esketamine for the rapid reduction of symptoms of depression and suicidality in patients at imminent risk for suicide: results of a double-blind, randomized, placebo-controlled study. Am. J. Psychiatry 175, 620–630.

Chen, X., Shu, S., and Bayliss, D.A. (2009). HCN1 channel subunits are a molecular substrate for hypnotic actions of ketamine. J. Neurosci. 29, 600–609.

Daly, E.J., Trivedi, M.H., Janik, A., Li, H., Zhang, Y., Li, X., Lane, R., Lim, P., Duca, A.R., Hough, D., et al. (2019). Efficacy of esketamine nasal spray plus oral antidepressant treatment for relapse prevention in patients with treatment-resistant depression: a randomized clinical trial. JAMA Psychiatry 76, 893–903.

Fava, M., Freeman, M.P., Flynn, M., Judge, H., Hoeppner, B.B., Cusin, C., Ionescu, D.F., Mathew, S.J., Chang, L.C., Iosifescu, D.V., et al. (2018). Double-blind, placebo-controlled, dose-ranging trial of intravenous ketamine as adjunctive therapy in treatment-resistant depression (TRD). Mol. Psychiatry. https://doi.org/10.1038/s41380-018-0256-5.

Ferrari, A.J., Somerville, A.J., Baxter, A.J., Norman, R., Patten, S.B., Vos, T., and Whiteford, H.A. (2013). Global variation in the prevalence and incidence of major depressive disorder: a systematic review of the epidemiological literature. Psychol. Med. 43, 471–481.

Hoffman, D.A., and Johnston, D. (1998). Downregulation of transient K+ channels in dendrites of hippocampal CA1 pyramidal neurons by activation of PKA and PKC. J. Neurosci. 18, 3521–3528.

Iijima, M., Fukumoto, K., and Chaki, S. (2012). Acute and sustained effects of a metabotropic glutamate 5 receptor antagonist in the novelty-suppressed feeding test. Behav. Brain Res. 235, 287–292.

Karst, H., Karten, Y.J., Reichardt, H.M., de Kloet, E.R., Schutz, G., and Joels, M. (2000). Corticosteroid actions in hippocampus require DNA binding of glucocorticoid receptor homodimers. Nat. Neurosci. 3, 977–978.

Kerr, D.S., Campbell, L.W., Thibault, O., and Landfield, P.W. (1992). Hippocampal glucocorticoid receptor activation enhances voltage-dependent Ca2+ conductances: relevance to brain aging. Proc. Natl. Acad. Sci. U S A 89, 8527–8531.

Kersten, M., Rabbe, T., Blome, R., Porath, K., Sellmann, T., Bien, C.G., Kohling, R., and Kirschstein, T. (2019). Novel object recognition in rats with NMDAR dysfunction in CA1 after stereotactic injection of anti-NMDAR encephalitis cerebrospinal fluid. Front. Neurol. 10, 586.

Kim, C.S., Brager, D.H., and Johnston, D. (2018). Perisomatic changes in h-channels regulate depressive behaviors following chronic unpredictable stress. Mol. Psychiatry 23, 892–903.

Kim, C.S., Chang, P.Y., and Johnston, D. (2012). Enhancement of dorsal hippocampal activity by knockdown of HCN1 channels leads to anxiolytic- and antidepressant-like behaviors. Neuron 75, 503–516.

Kim, C.S., and Johnston, D. (2015). A1 adenosine receptor-mediated GIRK channels contribute to the resting conductance of CA1 neurons in the dorsal hippocampus. J. Neurophysiol. 113, 2511–2523.

Kim, C.S., and Johnston, D. (2018). A possible link between HCN channels and depression. Chronic Stress (Thousand Oaks) 2, 1–6.

Koike, H., Fukumoto, K., Iijima, M., and Chaki, S. (2013). Role of BDNF/TrkB signaling in antidepressant-like effects of a group II metabotropic glutamate receptor antagonist in animal models of depression. Behav. Brain Res. 238, 48–52.

Li, N., Lee, B., Liu, R.J., Banasr, M., Dwyer, J.M., Iwata, M., Li, X.Y., Aghajanian, G., and Duman, R.S. (2010). mTOR-dependent synapse formation underlies the rapid antidepressant effects of NMDA antagonists. Science 329, 959–964.

Lodge, D., and Mercier, M.S. (2015). Ketamine and phencyclidine: the good, the bad and the unexpected. Br. J. Pharmacol. 172, 4254–4276.

Lorincz, A., Notomi, T., Tamas, G., Shigemoto, R., and Nusser, Z. (2002). Polarized and compartment-dependent distribution of HCN1 in pyramidal cell dendrites. Nat. Neurosci. 5, 1185–1193.

Lumsden, E.W., Troppoli, T.A., Myers, S.J., Zanos, P., Aracava, Y., Kehr, J., Lovett, J., Kim, S., Wang, F.H., Schmidt, S., et al. (2019). Antidepressant-relevant concentrations of the ketamine metabolite (2R,6R)-hydroxynorketamine do not block NMDA receptor function. Proc. Natl. Acad. Sci. U S A 116, 5160–5169.

Maeng, S., Zarate, C.A., Jr., Du, J., Schloesser, R.J., Mccammon, J., Chen, G., and Manji, H.K. (2008). Cellular mechanisms underlying the antidepressant effects of ketamine: role of alpha-

amino-3-hydroxy-5-methylisoxazole-4-propionic acid receptors. Biol. Psychiatry 63, 349–352.

Magee, J.C. (1998). Dendritic hyperpolarization-activated currents modify the integrative properties of hippocampal CA1 pyramidal neurons. J. Neurosci. 18, 7613–7624.

Magee, J.C. (1999). Dendritic Ih normalizes temporal summation in hippocampal CA1 neurons. Nat. Neurosci. 2, 508–514.

Malik, R., and Johnston, D. (2017). Dendritic GIRK channels gate the integration window, plateau potentials, and induction of synaptic plasticity in dorsal but not ventral CA1 neurons. J. Neurosci. 37, 3940–3955.

Mayberg, H.S., Brannan, S.K., Tekell, J.L., Silva, J.A., Mahurin, R.K., Mcginnis, S., and Jerabek, P.A. (2000). Regional metabolic effects of fluoxetine in major depression: serial changes and relationship to clinical response. Biol. Psychiatry 48, 830–843.

Mayberg, H.S., Lozano, A.M., Voon, V., Mcneely, H.E., Seminowicz, D., Hamani, C., Schwalb, J.M., and Kennedy, S.H. (2005). Deep brain stimulation for treatment-resistant depression. Neuron 45, 651–660.

Mcgowan, J.C., Lagamma, C.T., Lim, S.C., Tsitsiklis, M., Neria, Y., Brachman, R.A., and Denny, C.A. (2017). Prophylactic ketamine attenuates learned fear. Neuropsychopharmacology 42, 1577–1589.

Monteggia, L.M., Eisch, A.J., Tang, M.D., Kaczmarek, L.K., and Nestler, E.J. (2000). Cloning and localization of the hyperpolarization-activated cyclic nucleotide-gated channel family in rat brain. Brain Res. Mol. Brain Res. 81, 129–139.

Narayanan, R., Dougherty, K.J., and Johnston, D. (2010). Calcium store depletion induces persistent perisomatic increases in the functional density of h channels in hippocampal pyramidal neurons. Neuron 68, 921–935.

Narayanan, R., and Johnston, D. (2007). Long-term potentiation in rat hippocampal neurons is accompanied by spatially widespread changes in intrinsic oscillatory dynamics and excitability. Neuron 56, 1061–1075.

Preskorn, S.H., Baker, B., Kolluri, S., Menniti, F.S., Krams, M., and Landen, J.W. (2008). An innovative design to establish proof of concept of the antidepressant effects of the NR2B subunit selective N-methyl-D-aspartate antagonist, CP-101,606, in patients with treatment-refractory major depressive disorder. J. Clin. Psychopharmacol. 28, 631–637.

Rosenkranz, J.A., Venheim, E.R., and Padival, M. (2010). Chronic stress causes amygdala hyperexcitability in rodents. Biol. Psychiatry 67, 1128–1136.

Silveira Villarroel, H., Bompolaki, M., Mackay, J.P., Miranda Tapia, A.P., Michaelson, S.D., Leitermann, R.J., Marr, R.A., Urban, J.H., and Colmers, W.F. (2018). NPY induces stress resilience via downregulation of Ih in principal neurons of rat basolateral amygdala. J. Neurosci. 38, 4505–4520.

Suzuki, K., Nosyreva, E., Hunt, K.W., Kavalali, E.T., and Monteggia, L.M. (2017). Effects of a ketamine metabolite on synaptic NMDAR function. Nature 546, E1–E3.

Wang, J., Chen, S., and Siegelbaum, S.A. (2001). Regulation of hyperpolarization-activated HCN channel gating and cAMP modulation due to interactions of COOH terminus and core transmembrane regions. J. Gen. Physiol. 118, 237–250.

Williams, N.R., Heifets, B.D., Blasey, C., Sudheimer, K., Pannu, J., Pankow, H., Hawkins, J., Birnbaum, J., Lyons, D.M., Rodriguez, C.I., and Schatzberg, A.F. (2018). Attenuation of antidepressant effects of ketamine by opioid receptor antagonism. Am. J. Psychiatry 175, 1205–1215.

Wray, N.H., Schappi, J.M., Singh, H., Senese, N.B., and Rasenick, M.M. (2018). NMDAR-independent, cAMP-dependent antidepressant actions of ketamine. Mol. Psychiatry 24, 1833–1843.

Zanos, P., Moaddel, R., Morris, P.J., Georgiou, P., Fischell, J., Elmer, G.I., Alkondon, M., YUAN, P., Pribut, H.J., Singh, N.S., et al. (2016). NMDAR inhibition-independent antidepressant actions of ketamine metabolites. Nature 533, 481–486.

Zarate, C.A., Jr., Singh, J.B., Carlson, P.J., Brutsche, N.E., Ameli, R., Luckenbaugh, D.A., Charney, D.S., and Manji, H.K. (2006a). A randomized trial of an N-methyl-D-aspartate antagonist in treatment-resistant major depression. Arch. Gen. Psychiatry 63, 856–864.

Zarate, C.A., Jr., Singh, J.B., Quiroz, J.A., de Jesus, G., Denicoff, K.K., Luckenbaugh, D.A., Manji, H.K., and Charney, D.S. (2006b). A double-blind, placebo-controlled study of memantine in the treatment of major depression. Am. J. Psychiatry 163, 153–155.

Supplemental Information

Antidepressant Effects of (S)-Ketamine

through a Reduction

of Hyperpolarization-Activated Current I$_h$
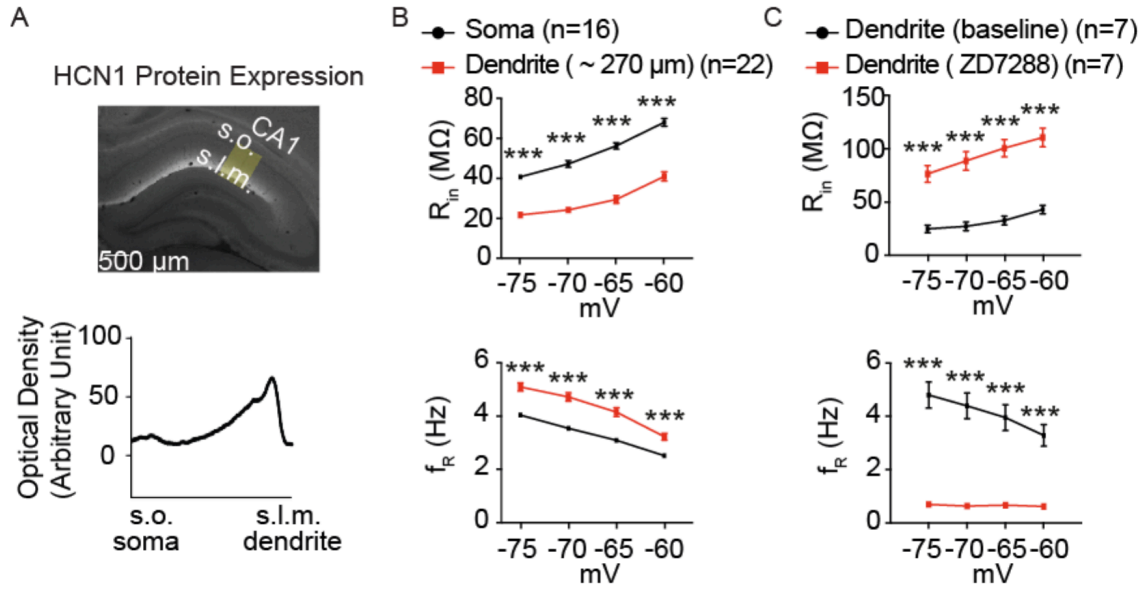
Chung Sub Kim and Daniel Johnston

Figure S1. Distance-dependent increases in I_h-sensitive electrophysiological measurements of dorsal CA1 region/neurons, Related to Figure 1. (A) HCN1 protein expression is a distance-dependent increase along the somatodendritic axis of dorsal CA1 region. (B) Dendritic region of CA1 neurons had a lower R_{in} and a higher f_R compared to somatic region of CA1 neurons. ***p<0.001 by two-way ANOVA with Sidark's multiple comparisons test. (C) ZD7288 (10 µM), a HCN channel blocker, increased dendritic R_{in} and removed dendritic f_R compared to baseline. ***p<0.001 by two-way ANOVA with Sidark's multiple comparisons test. Data are expressed as mean ± SEM.
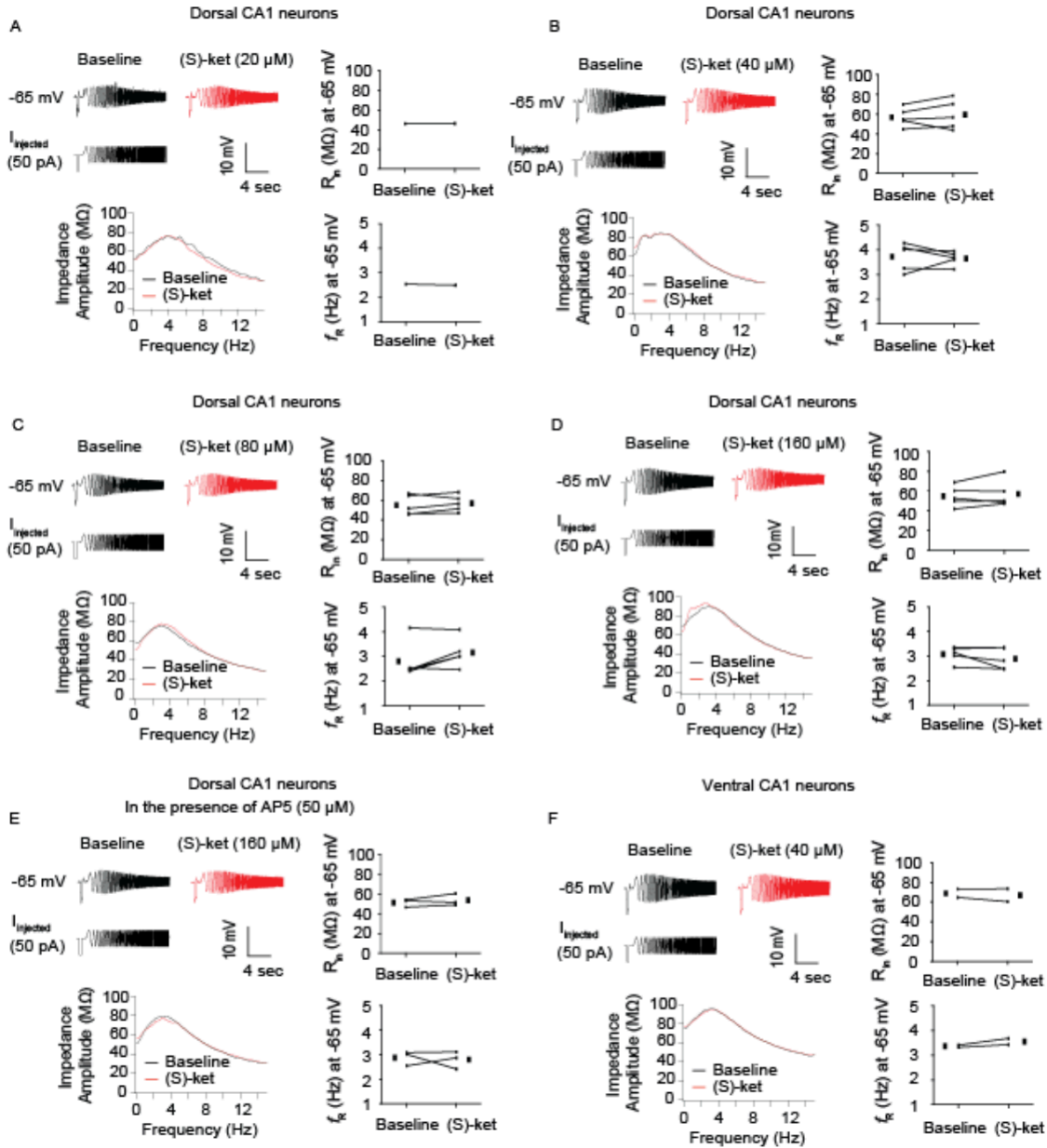
Figure S2. No changes in somatic I_h-sensitive measurements following four different concentrations of (S)-ketamine in dorsal or ventral CA1 neurons with or without AP5 (50 µM), Related to Figure 1. (A) 20 µM (S)-ketamine. (B) 40 µM (S)-ketamine. (C) 80 µM (S)-ketamine. (D) 160 µM (S)-ketamine. (E) 160 µM (S)-ketamine in the presence of AP5 (50 µM). (F) 40 µM (S)-ketamine in the ventral CA1 neurons. Data are expressed as mean ± SEM.
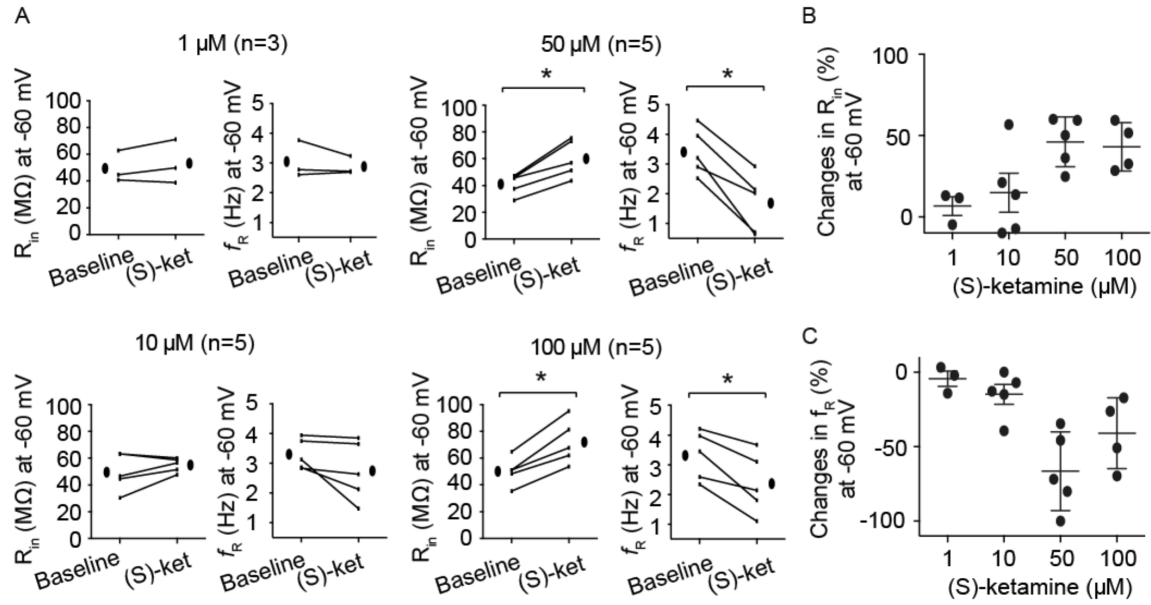
Figure S3. Dose-dependent effects of (S)-ketamine on dendritic I_h-sensitive measures of dorsal CA1 neurons, Related to Figure 1. (A-C) Dendritic R_{in} and f_R at multiple membrane potentials with different concentration of (S)-ketamine (1, 10, 50, and 100 µM). *p<0.05 by Wilcoxon matched-pairs signed rank test. Data are expressed as mean ± SEM.

A
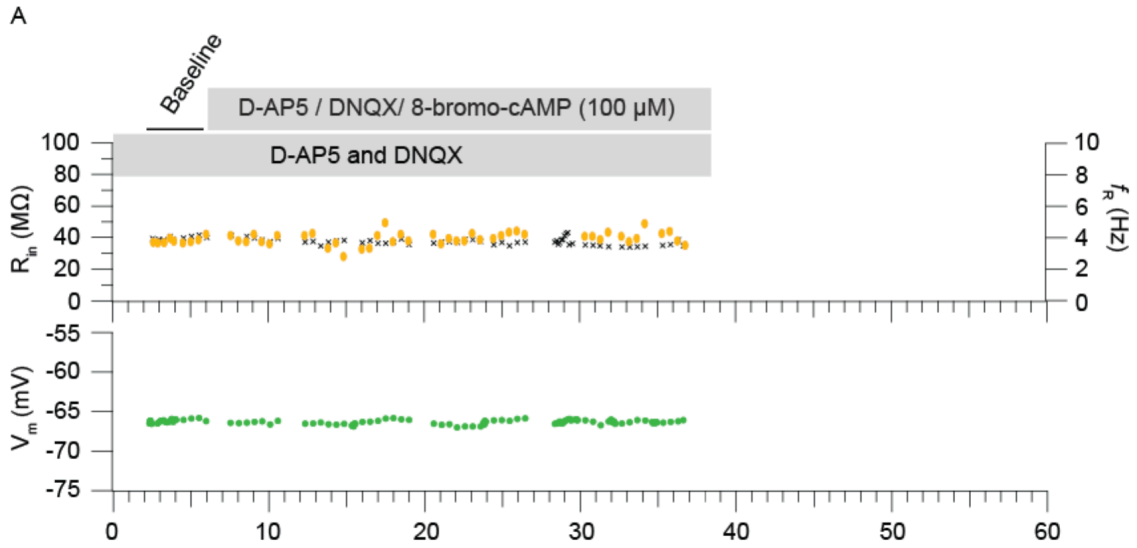
Figure S4. Time courses of V_m, R_{in}, and f_R in the presence of D-AP5 and DNQX following 8-bromo-cAMP application with dendrite recordings, Related to Figure 2.
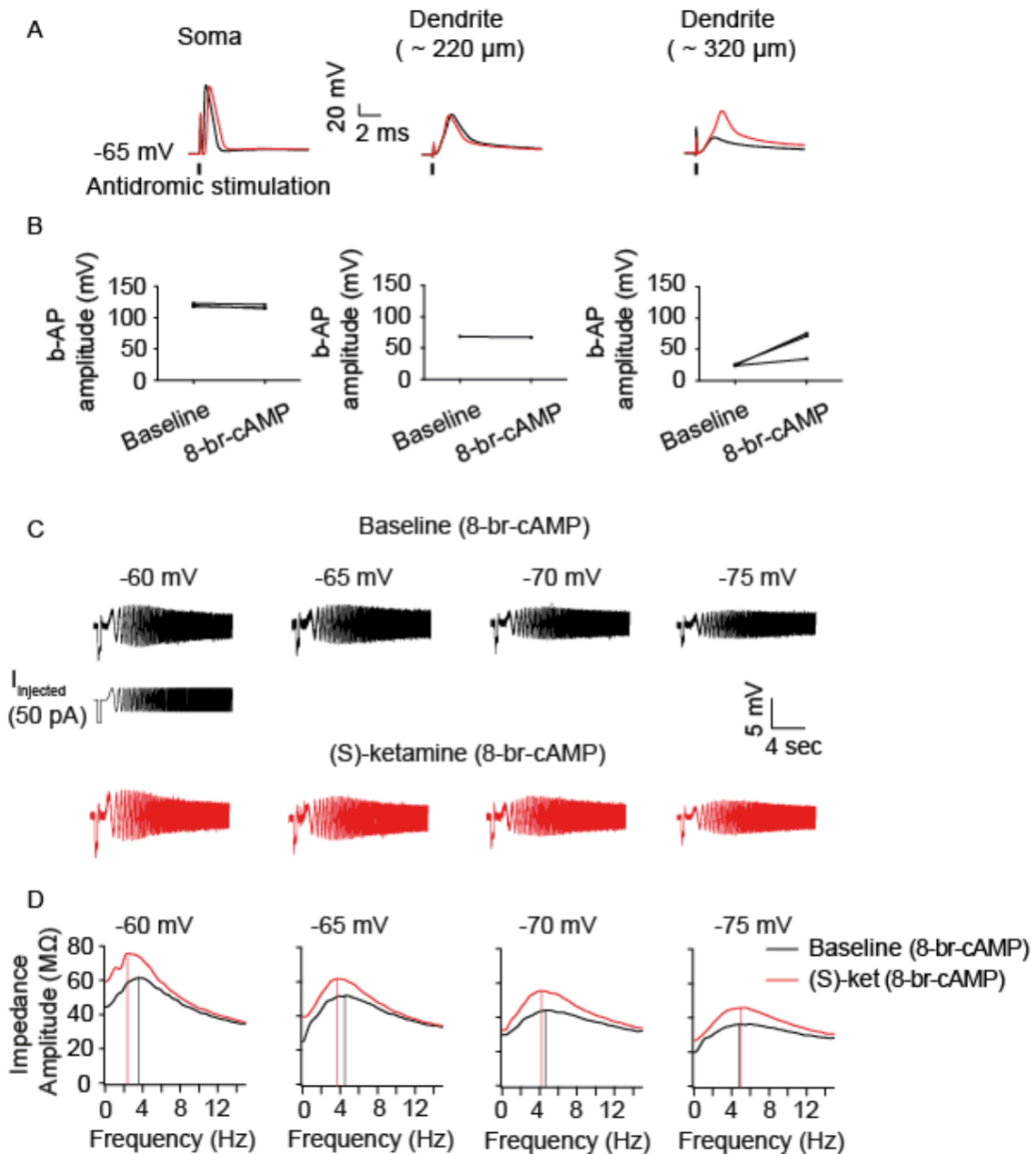
Figure S5. The effects of (S)-ketamine on dendritic I_h-sensitive electrophysiological measurements are independent of cAMP-dependent signaling, Related to Figure 2. (A) Representative voltage traces and antidromic stimulation at -65 mV. (B) Increased back-propagating action potentials (bAPs) amplitude at -65 mV in the distal dendrites of dorsal CA1 neurons following 8-bromo-cAMP (100 μM). (C) Representative voltage traces and current injections at different membrane potentials. (D) The profile of impedance amplitude for voltage traces in (C). Vertical lines indicate the resonance frequencies. Data are expressed as mean ± SEM.
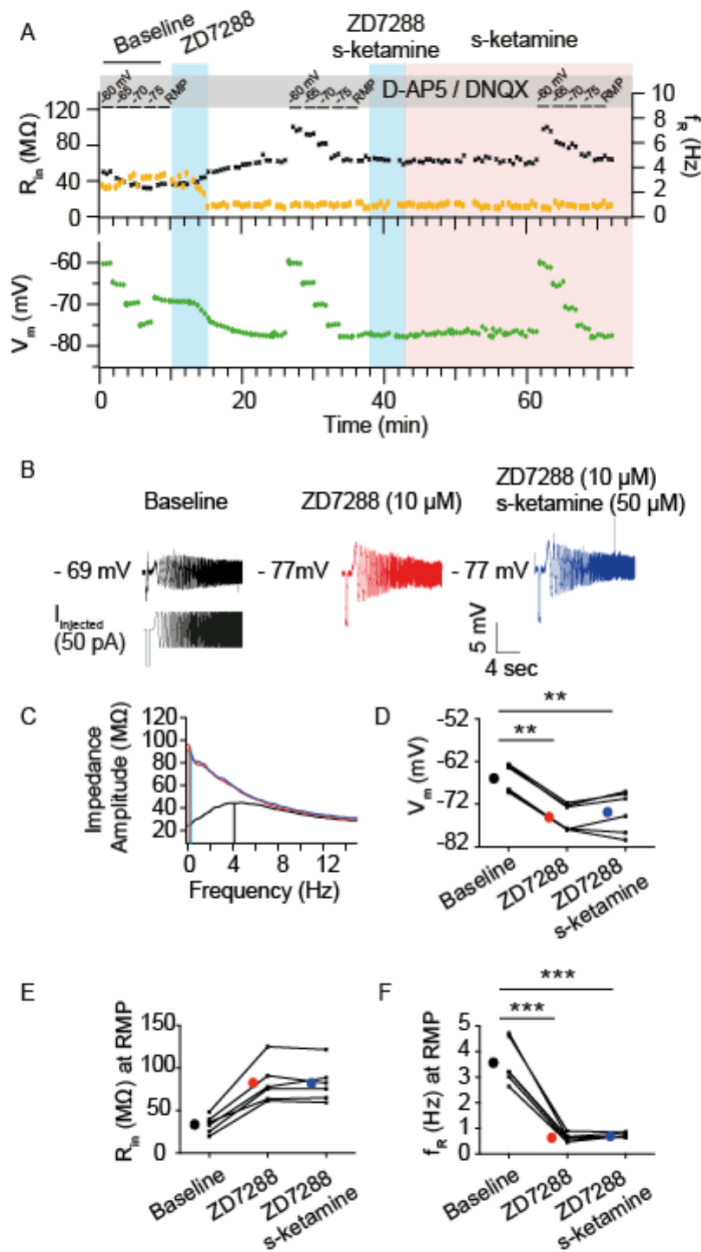
Figure S6. Occlusion effects of (S)-ketamine following ZD7288 application in the dorsal CA1 neurons, Related to Figure 2. (A) Time courses of changes in dendritic V_m, R_{in}, and f_R during successive ZD7288 (10 μM) and (S)-ketamine application in the dorsal CA1 neurons. (B) Representative voltage traces and current injections at resting membrane potential. (C) The profile of impedance amplitude for voltage traces in (B). (D-F) ZD7288 hyperpolarized V_m (D), increased R_{in} (E), and removed f_R (F). Addition of (S)-ketamine had no further effects on dendritic I_h-sensitive electrophysiological measurements (e.g. V_m, R_{in}, and f_R) at RMP. **p<0.01 and ***p<0.001 by One-way ANOVA with Tukey. Data are expressed as mean ± SEM.
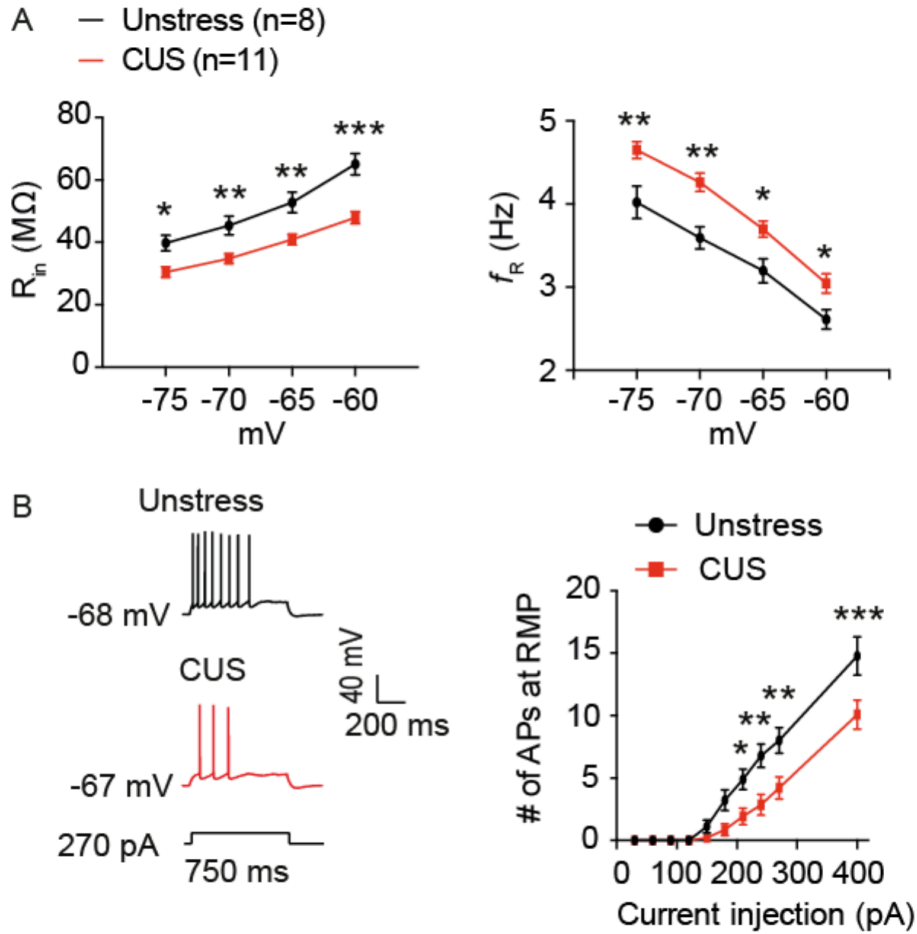
Figure S7. CUS-induced decrease in neuronal excitability, Related to Figure 5. (A) Dorsal CA1 neurons of CUS group showed a lower R_{in} and a high f_R at different membrane potentials compared with those from unstressed group. *$p<0.05$, **$p<0.01$, ***$p<0.001$ by two-way ANOVA with Sidark's multiple comparisons test. (B) Representative voltage responses with depolarizing current step (270 pA; 750 ms) at RMP. Action potential firing was significantly decreased in the dorsal CA1 neurons of CUS group compared with those from unstressed group. *$p<0.05$, **$p<0.01$, ***$p<0.001$ by two-way ANOVA with Sidark's multiple comparisons test. Data are expressed as mean ± SEM.
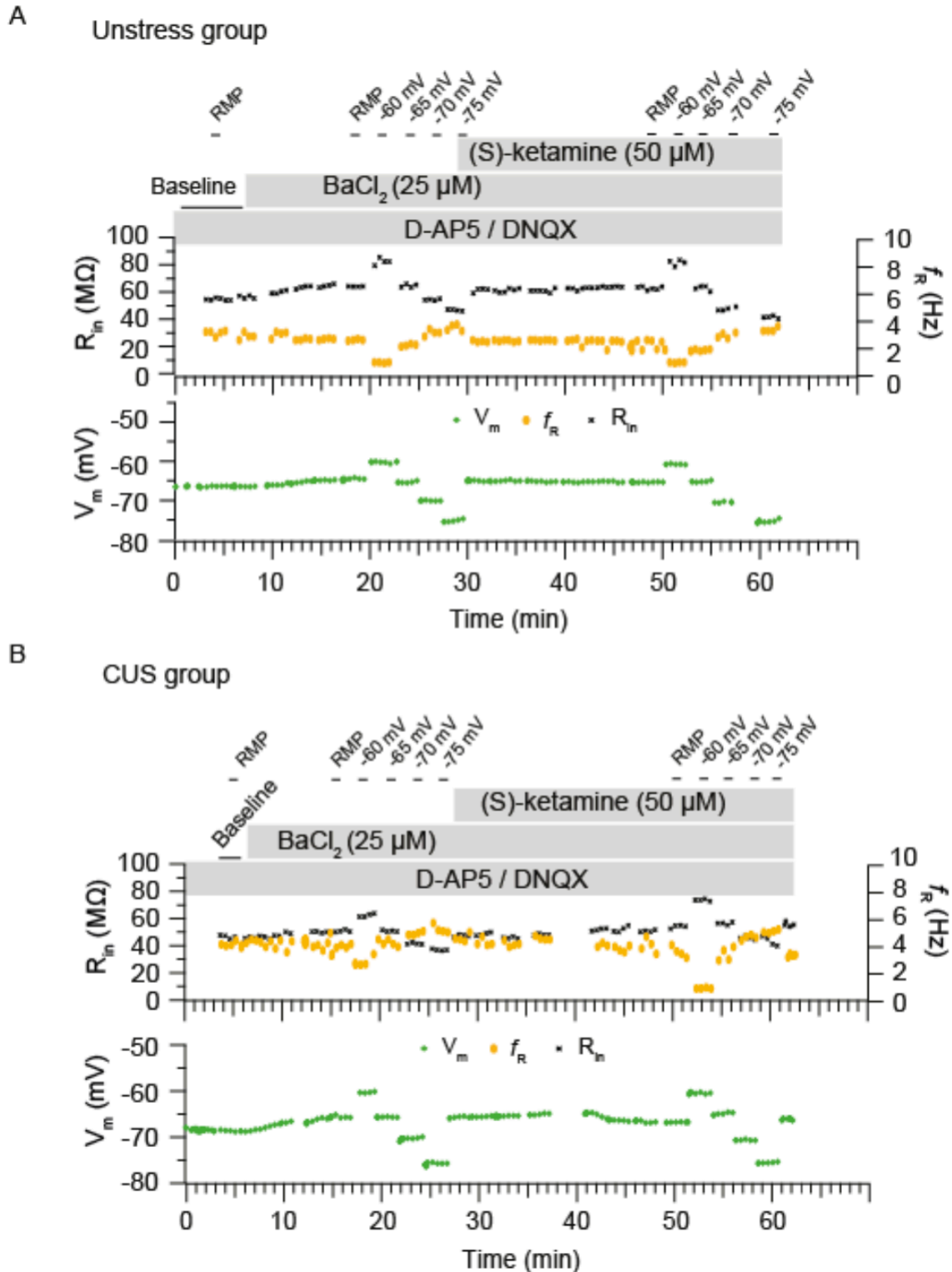
Figure S8. Time courses of changes in V_m, R_{in}, and f_R in the presence of D-AP5 and DNQX during successive $BaCl_2$ and (S)-ketamine applications in unstress (A) and CUS groups (B), Related to Figure 5.
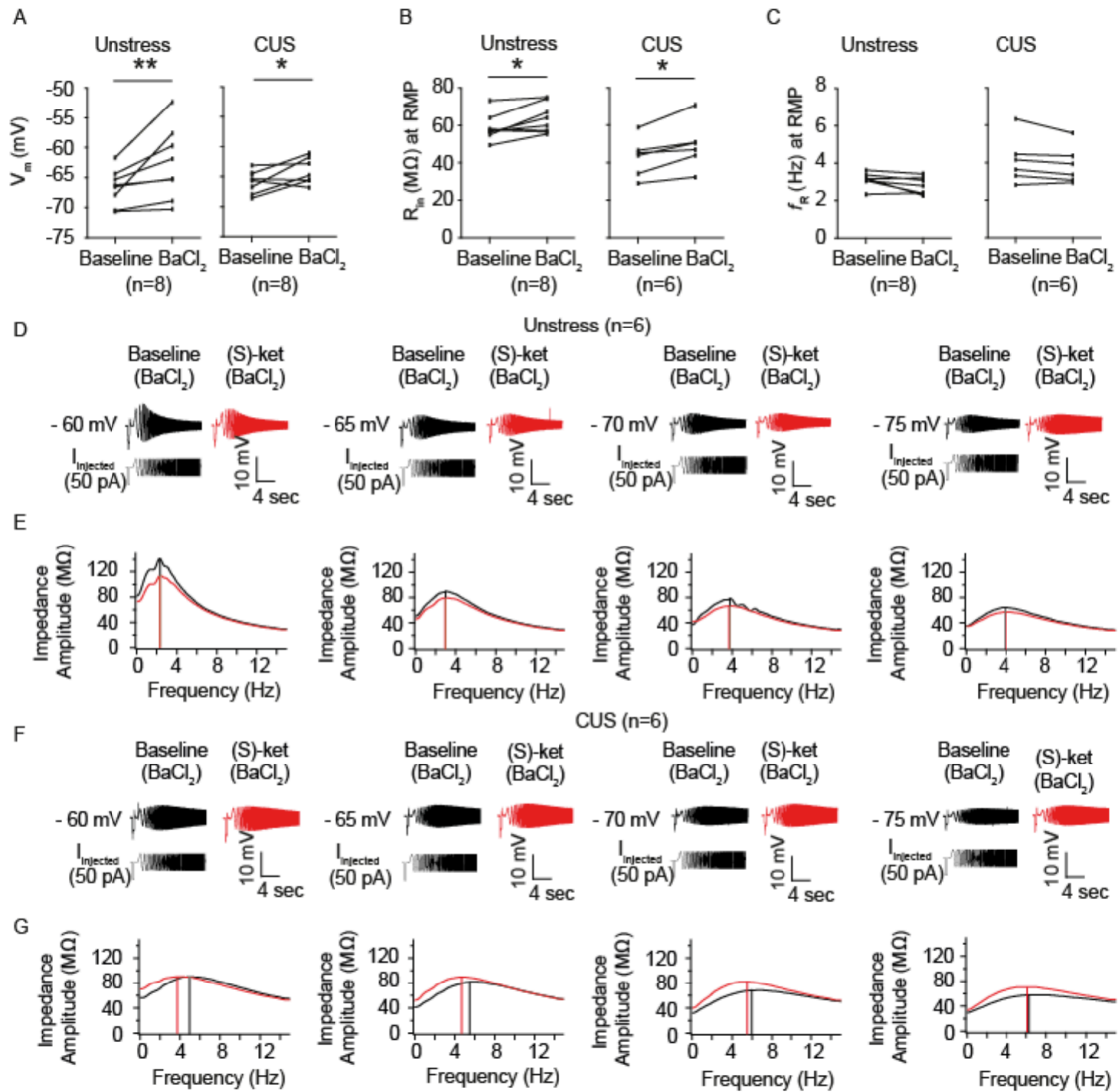
Figure S9. The effects of (S)-ketamine on CUS-induced upregulation of somatic I_h-sensitive electrophysiological measurements were independent of barium-sensitive conductance, Related to Figure 5. (A-C) A low concentration of barium (25 μM) depolarized RMP (A) and increased R_{in} (B), whereas f_R (C) was not altered in the dorsal CA1 neurons of unstressed and CUS groups. *p<0.05, **p<0.01 by Wilcoxon matched-pairs signed rank test. (D and F) Representative voltage traces and current injections at different membrane potentials in unstressed (D) and CUS (F) groups. (E and G) The profile of impedance amplitude for voltage traces in (D and F respectively). Vertical lines indicate the resonance frequencies. Data are expressed as mean ± SEM.
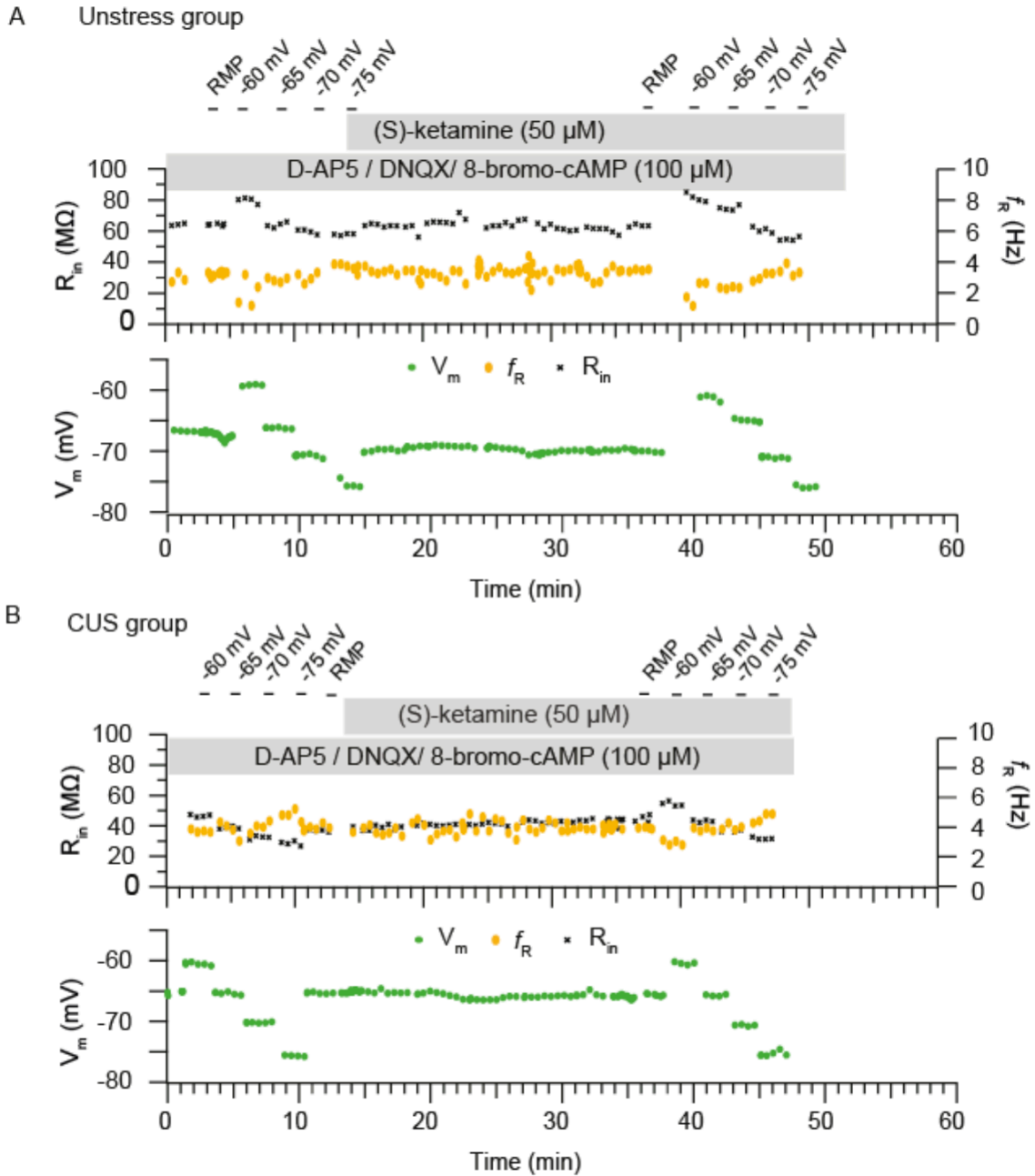
Figure S10. Time courses of changes in V_m, R_{in}, and f_R in the presence of D-AP5, DNQX, and 8-bromo-cAMP during (S)-ketamine application in unstress (A) and CUS groups (B), Related to Figure 5.
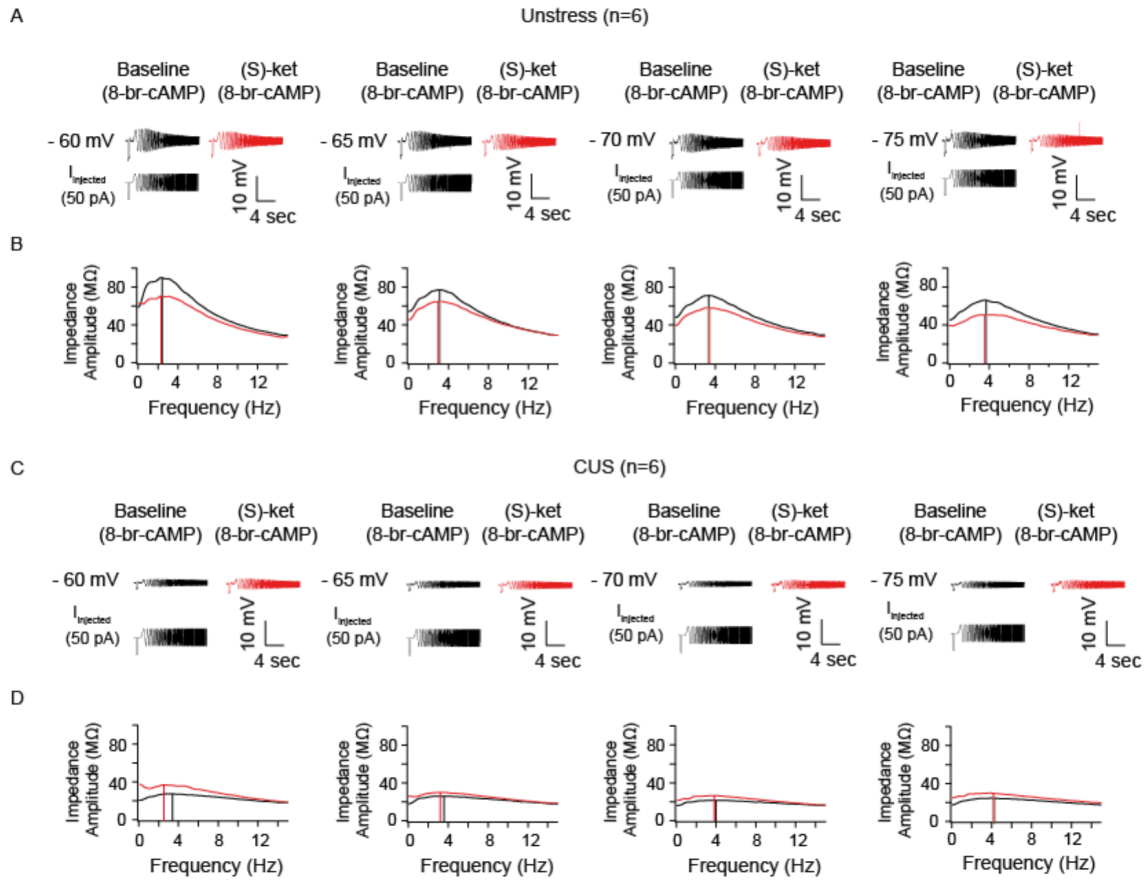
Figure S11. The effects of (S)-ketamine on CUS-induced upregulation of I_h-sensitive electrophysiological measurements were independent of cAMP-dependent signaling, Related to Figure 5. (A and C) Representative voltage traces and current injections at different membrane potentials in unstressed (A) and CUS (C) groups. (B and D) The profile of impedance amplitude for voltage traces in (A and C respectively). Vertical lines indicate the resonance frequencies. Data are expressed as mean ± SEM.

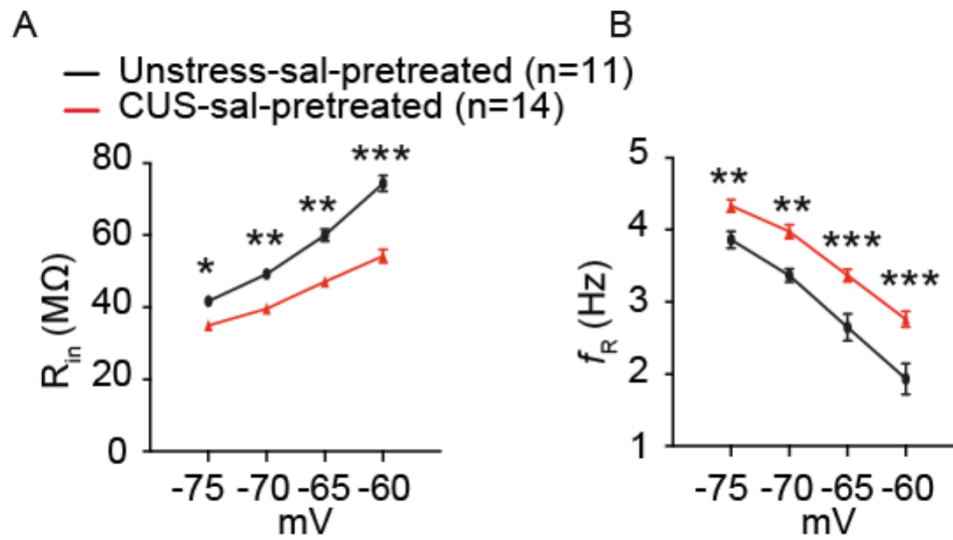Figure S12. Dorsal CA1 neurons from the saline-pretreated CUS group showed a lower R_{in} (A) and a high f_R (B) at different membrane potentials compared with those from unstressed group, Related to Figure 9. *p<0.05, **p<0.01, ***p<0.001 by two-way ANOVA with Sidark's multiple comparisons test. Data are expressed as mean ± SEM.
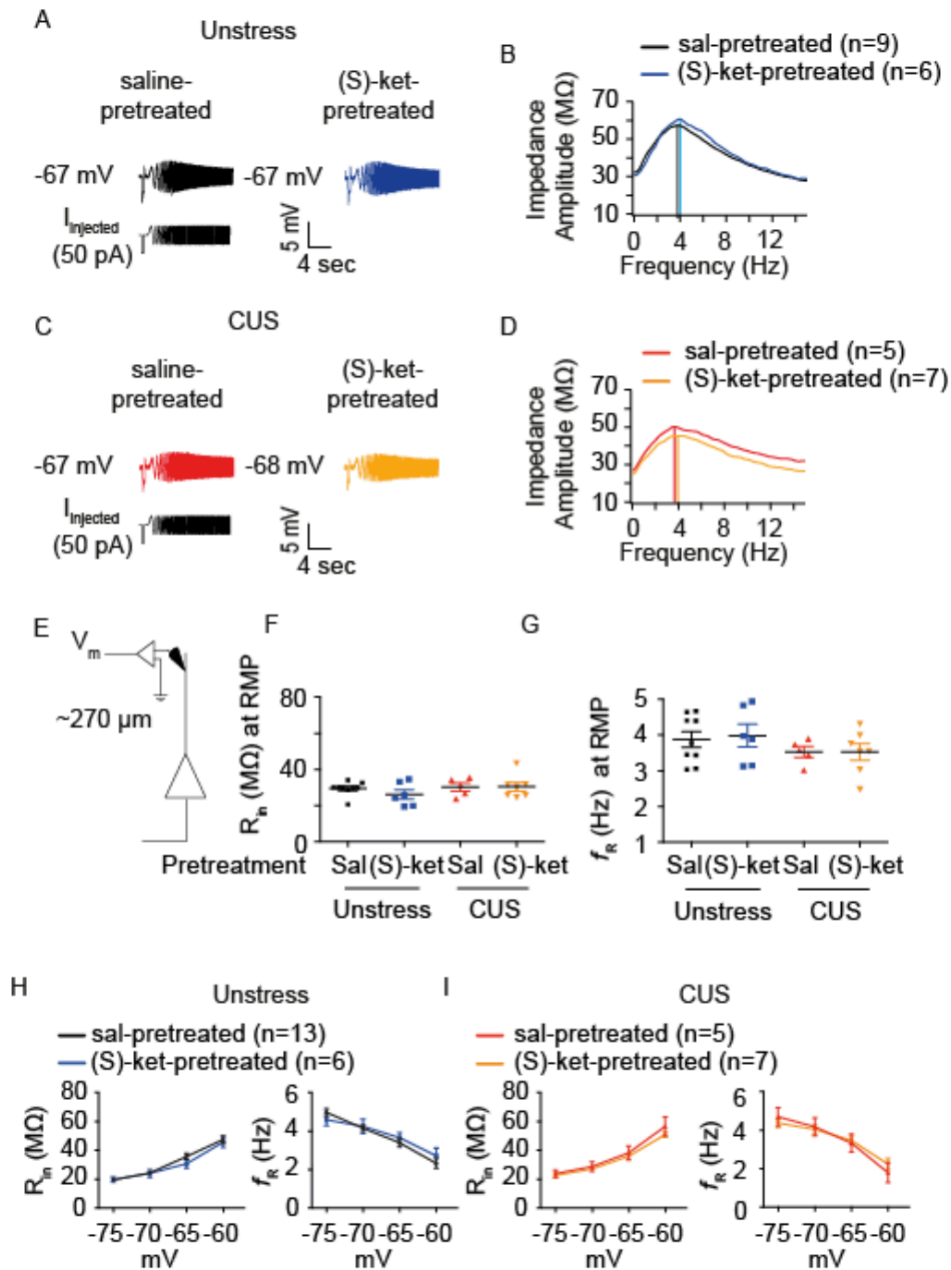
Figure S13. There were no changes in dendritic I_h-sensitive electrophysiological measurements between groups (unstressed *vs.* CUS groups; saline- *vs.* (S)-ketamine-pretreated groups), Related to Figure 9. (A and C) Representative voltage traces and current injections at RMP. (B and D) The profile of impedance amplitude for voltage traces in (A and C). Vertical lines indicate the resonance frequencies. (E) Schematic of the somato-apical trunk depicting the dendritic recordings. There were no different dendritic R_{in} and f_R between groups at RMP (F and G) and at different membrane potentials (H and I). Data are expressed as mean ± SEM.
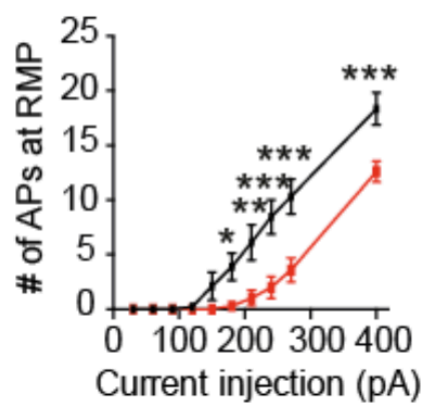
Figure S14. Saline-pretreated CUS group showed decreased neuronal excitability, Related to Figure 10. Action potential firing was significantly lowered in the dorsal CA1 neurons of saline-pretreated CUS group compared with those from unstressed group. *p<0.05, **p<0.01, ***p<0.001 by two-way ANOVA with Sidark's multiple comparisons test. Data are expressed as mean ± SEM.

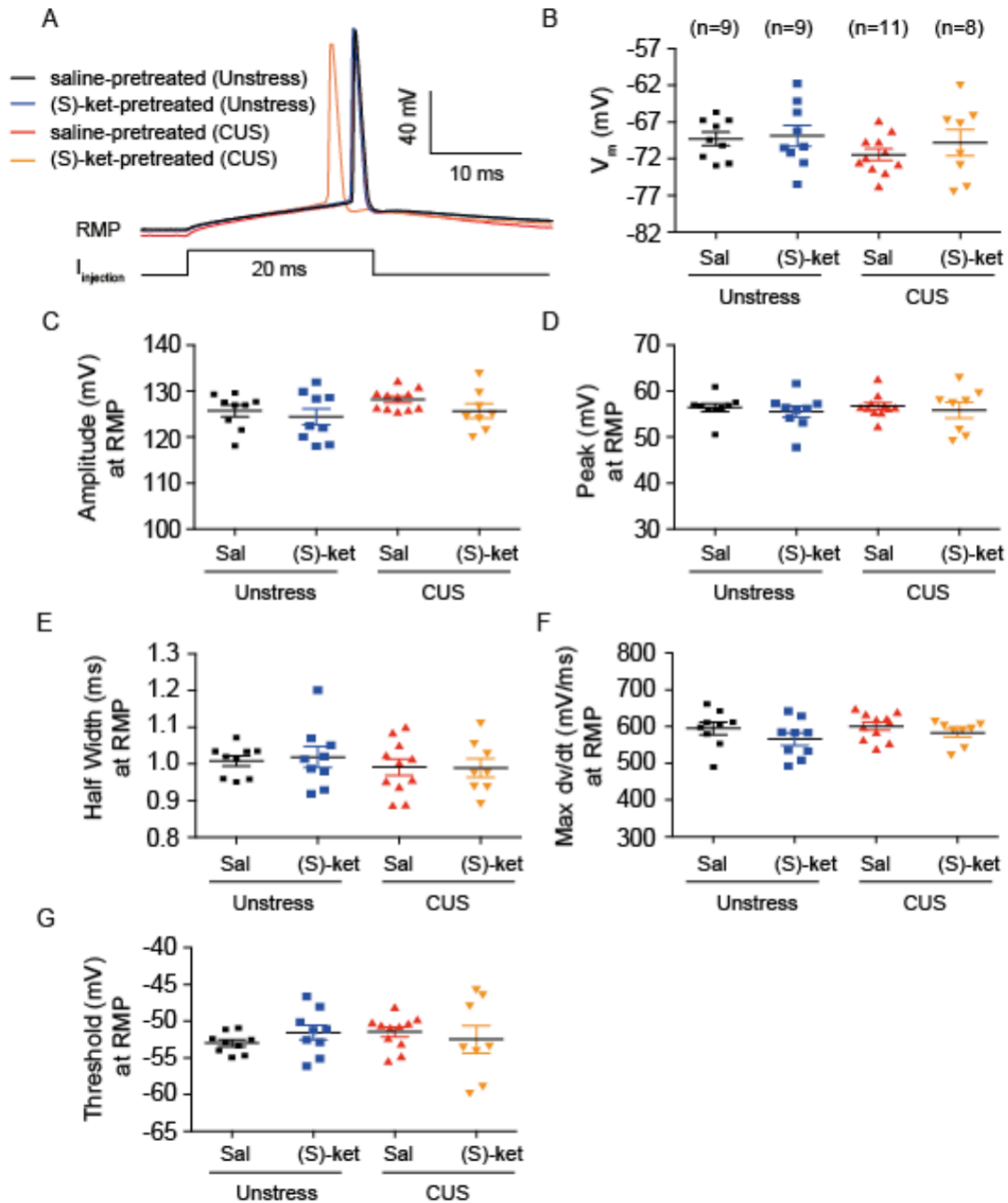Figure S15. Action potential firing properties in (S)-ketamine-pretreated in unstressed and CUS groups, Related to Figure 10. (A) Representative traces and current injections at RMP. (B – G) V_m (B), amplitude (C), peak (D), half-width (E), max dv/dt (F), and threshold (G) were not different between unstressed (sal- or (S)-ket-pretreated) and CUS (sal- or (S)-ket-pretreated) groups. Data are expressed as mean ± SEM.
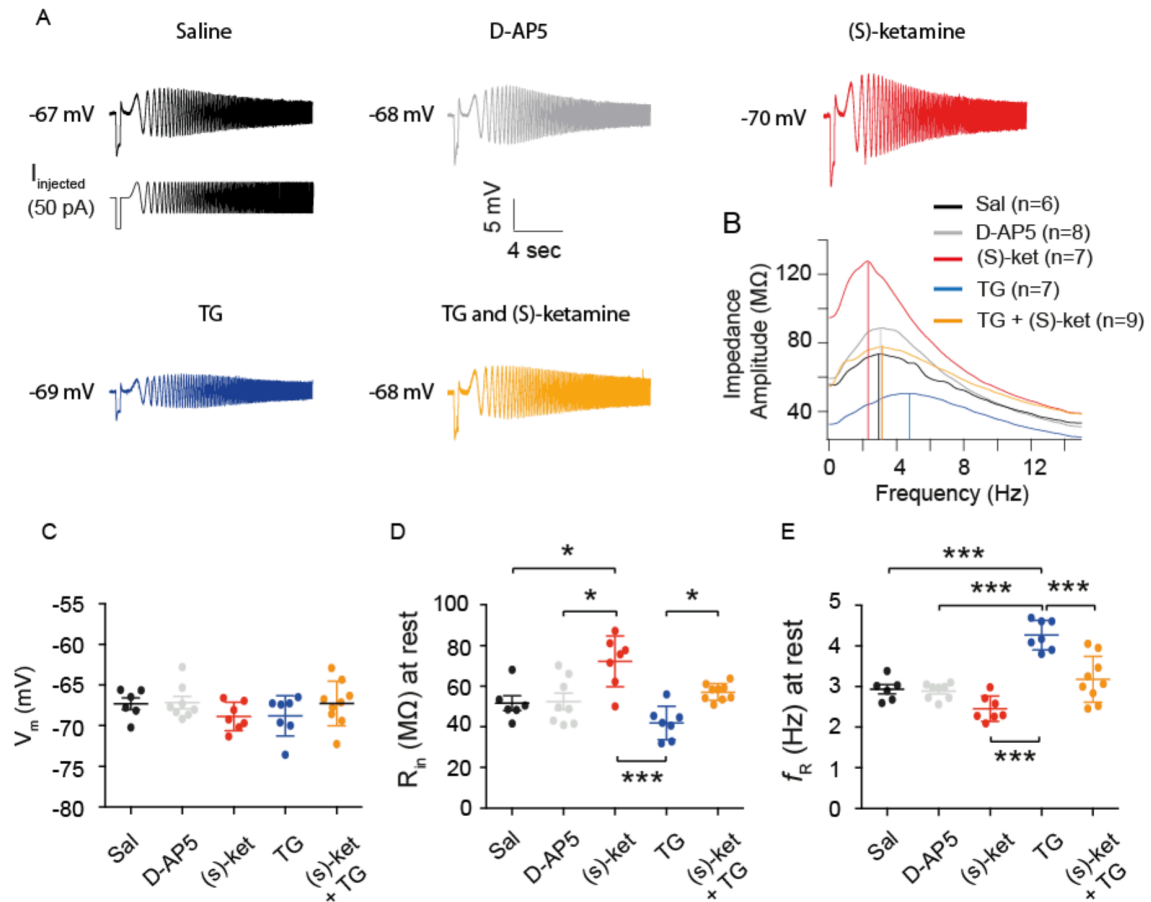
Figure S16. *In vivo* infusion of TG-induced upregulation of functional I_h was reversed by (S)-ketamine in dorsal CA1 region, Related to Figure 12. (A) Representative voltage traces and current injections at RMP. (B) The profile of impedance amplitude for voltage traces in (A). Vertical lines indicate the resonance frequencies. (C) There were no significant differences in RMP between groups. (D and E) Dorsal CA1 neurons of (S)-ketamine-infused group showed decreased functional I_h, whereas increased functional I_h from TG-infused group. Dorsal CA1 neurons of TG+(S)-ketamine-infused group showed decreased functional I_h. *$p<0.05$ and ***$p<0.001$ by One-way ANOVA with Tukey. Data are expressed as mean ± SEM.

Transparent Methods

Animals

Male Sprague-Dawley rats (CUS procedures: 7- to 9-week old rats, behavioral and electrophysiological tests: 9-to-14-week old rats) were used in this study. Rats housed 2-3 per cage except for CUS-treated rats on a 12 hr light schedule (on 7:00 A.M. off 7:00 P.M.) with *ad libitum* access to water and food. All procedures involving animals were approved by the University of Texas at Austin Institutional Animal Care and Use Committee (IACUC).

Drugs

ZD7288 were purchased from Abcam Inc. D-APV, DNQX, and 8-bromo-cAMP were purchased from Tocris. S-ketamine was obtained from Sigma-Aldrich Co. Barium chloride was purchased from Fisher Scientific.

Chronic unpredictable stress (CUS) procedures

CUS procedure was carried out as previously described[19, 47]. Rats were housed 2-3 per cage throughout the experiment except when they were subjected to single housing, overcrowding, or behavioral testing. In chronic unpredictable stress, mild stressors were randomly administered once or twice daily at variable times of the day. Rats exposed to stress were kept in the procedure room for at least 1-2 hr until odor from the stress procedure disappeared. The body weight of the rats was measured during the CUS procedure. CUS rats were kept under stress procedure until electrophysiological recordings were done.

Behavioral tests

Sucrose preference test, open field test, and forced swim test were performed as previously described[17, 19].

- **Sucrose preference test.** After the sequential application of a variety of mild stressors

for 2 to 3 weeks, CUS-treated and handled control rats habituated to two water bottles for 2 days in their home cages. After the 2-day habituation, CUS-treated and handled control rats were housed in single cages to test for sucrose preference (1% sucrose). The positions of bottles were counterbalanced across the left or right side of the testing cages. Water intake and 1% sucrose intake were measured during a 12 hr dark-cycle. Sucrose preference was determined as the ratio of sucrose to total water consumption.

- Open field test. Each rat was randomly assigned and placed into the center of the field. Animals in the open field arena were recorded for 6 min using a CCD camera. After each testing session, the apparatus was cleaned with 70% EtOH to remove any odors deposited by previous animals. Total travelled distance and center square entries were measured using a custom written program. A line crossing was defined when the body center crosses a line.

- Forced swim test. Each rat was placed in a transparent Plexiglas cylinder (80 cm tall x 30 cm in diameter) filled with water (23–24 °C) to a depth of 45 cm. Water in the tank was changed after each trial. For pretest session (day 1), rats without any drug treatments were placed in the water for 15 min. Rats were placed in the water again for a 6 min (test session) 24 hr after the pretest session. The behaviors in the forced swim test were recorded by a video cameras positioned on the top of the water tank. Passive activity was defined as floating and making only those movements necessary to keep the nose above the water. Behaviors from the forced swim test was quantified using a custom written program that used a time sampling technique to rate the predominant behavior over a 5-sec interval as previously described [48].

Dorsal CA1 cannulation and infusion.

Dorsal CA1 cannulation and infusion were performed as previously described[19]. Male Sprague-Dawley rats weighing 200-225 g were anesthetized by an intraperitoneal

injection of a mixture of ketamine/xylazine (90/10 mg ml^{-1}; 0.1 ml per 100 g rat intraperitoneally). A stainless steel guide cannula (22 gauge; P1 Technologies, Roanoke, VA, USA) was bilaterally implanted 1 mm above the dorsal CA1 region (AP: − 3.8 mm, ML: ± 2.5 mm, DV: − 1.4 mm) and secured with screws in the skull and dental acrylic cement. After stereotaxic implantation, a dummy cannula (P1 Technologies) was inserted into each guide cannula to maintain patency. Rats received food soaked with Baytril (0.3 ml; Bayer, Shawnee Mission, KS, USA), an antibiotic as prophylaxis against infection as well as triple antibiotic ointment (Select Medical Product) applied around the surgery areas. After a minimum 5-day recovery period, rats were divided into five groups: 1) saline, 2) D-AP5 (25 µM), 3) (S)-ketamine (50 µM) with D-AP5 (25 µM), 4) TG (1 µM) with D-AP5 (25 µM), and 5) subsequent infusion of TG (1 µM) with D-AP5 and (S)-ketamine (50 µM) with D-AP5 (25 µM). All infusions (1 µl per side for 5 min) were performed in their home cages 40 - 50 min before the open field test. After completion of the infusion, the injector was left in place for 5 additional min before withdrawal. After a 10-min open field test, either sucrose preference test or acute dorsal hippocampal slice was performed.

Slice preparation

Rats were briefly exposed to isoflurane gas using soaked cotton pad in a closed plastic container. Then, rats were anesthetized with a lethal dose of a ketamine/xylazine mixture (90/10mg/ml; 0.2 - 0.3 ml/100 g rat i.p.) and transcardially perfused with ice-cold artificial cerebral spinal fluid (aCSF) composed of (in mM): 2.5 KCl, 1.25 NaH_2PO_4 , 25 $NaHCO_3$, 0.5 $CaCl_2$, 7 $MgCl_2$, 7 dextrose, 210 sucrose, 1.3 ascorbic acid, and 3 sodium pyruvate, bubbled with 95% O_2 - 5% CO_2. The brain was removed and hemisected along the longitudinal fissure. Dorsal hippocampal slices were prepared as previously described[19]. 300 µm thick hippocampal slices were made in ice-cold aCSF using a vibrating

microtome (Microslicer DTK-Zero1, DSK, Kyoto, Japan). Slices were placed in a holding chamber containing (in mM) 125 NaCl, 2.5 KCl, 1.25 NaH_2PO_4, 25 $NaHCO_3$, 2 $CaCl_2$, 2 $MgCl_2$, 12.5 dextrose, 1.3 ascorbic acid, and 3 sodium pyruvate, bubbled with 95% O_2 - 5% CO_2 at 35°C for 30 min and then incubated for at least 45 min at room temperature before used for electrophysiology.

Immunohistochemistry

Immunohistochemistry was carried out as described previously[19]. 300 μm thick slices were further sectioned using a freezing microtome into 40-μm thin sections and stored in cryoprotectant (30% sucrose, 30% ethylene glycol, 1% polyvinyl pyrrolidone, 0.05 M sodium phosphate buffer). Sections were briefly rinsed in PBS buffer and incubated in 0.1% TritonX-100 for 30 min. Subsequently, slices were blocked in PBS solution containing 5% normal goat serum, 0.03% TritonX-100 for 1hr, and then incubated in primary antibody diluted in blocking solution overnight at 4°C. Slices were rinsed in PBS buffer and then incubated in secondary antibody for 1hr at room temperature. Primary antibody in this study was the rabbit anti-HCN1 recognizing an epitope in the N-terminals of rat HCN1 (1:200, Alomone Labs).

Somatic and dendritic whole-cell current-clamp recordings

Whole-cell current-clamp recordings were performed as previously described.[17, 19, 22] Briefly, hippocampal slices were submerged in a recording chamber continuously perfused with aCSF containing (in mM) 125 NaCl, 3 KCl, 1.25 NaH_2PO_4, 25 $NaHCO_3$, 2 $CaCl_2$, 1 $MgCl_2$, and 12.5 dextrose, bubbled with 95% O_2 - 5% CO_2 at a rate of 1 ml/min and 31-33°C. All experiments were done in the presence of glutamatergic synaptic blockers (D-AP5 25 μM or 50 μM and DNQX 20 μM). CA1 pyramidal neurons were visually identified using a microscope (Zeiss Axioskop) fitted with differential interference contrast optics.[49] Patch pipettes for somatic (4–7 MΩ) and dendritic recordings (7-8 MΩ) were prepared with capillary glass (external diameter 1.65 mm and internal diameter 1.1

mm, World Precision Instruments) using a Flaming/Brown micropipette puller and filled with an internal solution containing (in mM) 120 K-gluconate, 20 KCl, 10 HEPES, 4 NaCl, 7 K2-phosphocreatine, 4 Mg-ATP, 0.3 Na-GTP (pH 7.3 with KOH). Whole-cell current-clamp recordings were performed using a Dagan BVC-700A amplifier (Dagan, Minneapolis, MN) and custom acquisition software written in IGOR Pro. Electrical signals were filtered at 5-10 kHz, sampled at 20-40 kHz, and digitized by an ITC-18 interface (Instructech Corporation, Port Washington, NY). Series resistance was monitored during each experiment and experiments were discarded if the series resistance exceeded 30 MΩ for somatic and dendritic recordings. The "natural" resting membrane potential was the potential of the soma or dendrite in the absence of any injected current. Liquid junction potential was not corrected and was estimated to be about -13 mV using the Patcher's Power Tools add-on in Igor Pro. All experiments were performed at 31°C – 33°C.

Cell-attached patch clamp recordings

For cell-attached recordings, pipettes contained the following (in mM): 120 KCl, 10 HEPES, 2.0 $CaCl_2$, 1.0 $MgCl_2$, 20 TEA-Cl, 0.2 3,4-diaminopyridine, 1 $BaCl_2$, pH 7.3 with KOH. Membrane currents were recorded using an Axopatch 200B amplifier (Molecular Devices), analog filtered at 1 kHz, and digitized at 10 kHZ by an ITC-18 interface connected to a computer running Axograph X. I_h was elicited by 500 ms voltage steps ranging from -40 mV to -170 mV in -10 mV increments from a holding potential of -30 mV. Maximal I_h amplitude was measured by using a hyperpolarizing voltage command to -170 mV from a holding potential of -30 mV. Linear leakage and capacitive currents were digitally subtracted by scaling traces at smaller command voltages in which no voltage-dependent current was activated. Between 350 and 400 individual leak traces were averaged in order to minimize the addition of noise to the leak subtracted current waveforms. All experiments were performed at 31°C – 33°C.

Data analysis. Sucrose preference (%) was calculated by dividing the total sucrose intake by the total fluid intake (plain water + 1% sucrose solution) for 12 hr (during the dark cycle). Input resistance was measured by the slope of the linear fit of the V-I plot between +10 and -150 pA current injections. Resonance frequency was measured as the frequency of the peak impedance using a sinusoidal current injection of constant amplitude and linearly spanning 0-15 Hz in 15 sec. h current was measured by the subtraction of the average amplitude of baseline (i.e., 10 ms to 90 ms before the step voltage) from the average amplitude of h current (i.e., 250 ms to 590 ms). Conductance was determined by $g(h) = I_h/(V - E_h)$, where V is the membrane potential (i.e., ranging from -40 to -170 mV) and E_h is the reversal potential for I_h (i.e., -10 mV). Normalized conductance was determined by $G = g_h/g_{h\ max}$. Normalized G-V relationships were described assuming a Boltzmann function: $G(V) = 1/[1+e^{(V-V_{1/2})/k}]$, where G(V) is the normalized conductance, V is the membrane potential, $V_{1/2}$ is the membrane potential associated with one-half of the maximal conductance value, and k is the slope factor.

Statistical Analysis. Statistical comparisons were performed using ANOVA (one-factor or two-factor) followed by Bonferrori post-hoc test, paired t test (Wilcoxon signed-rank test) or unpaired t test (Mann-Whitney U test) with GraphPad software.